

Global Stability Analysis of a Fractional-Order Ebola Epidemic Model with Control Strategies

Abstract

We proposed a fractional-order derivative model for Ebola virus disease (EVD) to assess the effects of control strategies on the spread of the disease in the population. The proposed model incorporates all relevant biological factors, health education campaigns, prevention measures, and treatment as control strategies. We computed the basic reproduction number \mathcal{R}_0 and qualitatively used it to assess the existence of the model states. In particular, we noted that two equilibrium points exist, the disease-free and endemic equilibrium points which are both globally stable whenever $\mathcal{R}_0 < 1$ and $\mathcal{R}_0 > 1$ respectively. We performed sensitivity analysis on the key parameters that drive the EVD dynamics to determine their relative importance in EVD transmission and prevalence. Model parameters were estimated using the 2014 Ebola outbreak in Guinea. Further, numerical simulation results are presented using fractional Adam-Bashforth-Moulton scheme to support the analytical findings. From the numerical simulations, we have noted that as α decreases from unit, the solution profiles of the model attain its stability much faster than at $\alpha = 1$. Furthermore, the results demonstrated that the aforementioned control strategies have the potential to reduce the transmission of EVD in the population.

Keywords: Lyapunov; Control Strategies; Ebola model; Fractional-order derivatives; Model stability; Data fitting; Model validation.

1 Introduction

Ebola virus disease (EVD) is a disease caused by Ebola virus in humans and other non-human primates like gorillas, chimpanzees and duikers. The virus originated in fruit bats and jumped to humans through animals such as chimpanzees [1, 2]. The disease first appeared in 1976 in two outbreaks, one in Sudan and the other in Democratic Republic of Congo (DRC). Since then, the disease has continued to appear in Africa several times, for example, in Ivory Coast and Gabon in 1994; in Uganda in 2000; in Guinea in 2014; and again in DRC in 2019.

The EVD outbreaks, particularly in Western part of Africa, continue to present substantial challenges to health and health-care resources in the region and beyond. According to the World Health organization (WHO), more than 11000 people died in the region between 2013 and 2016 due to the outbreak of EVD [3]. In particular, Sierra Leone alone recorded more than 14,100 Ebola cases which resulted in over 3900 deaths, and more than 30000 individuals were quarantined due to possible Ebola exposure [4].

Although several factors such as poor health facilities and highly populated urban areas have been attributed to perpetuate EVD during an outbreak, funeral and burial practices anchored in certain traditional and religious practices of the West African communities are regarded as one of the leading factors that fuel the spread of EVD in the region [5, 6]. As most communities in West Africa believe in life after death, funeral and burial practices are given a lot of significance and perceived as crucial steps in transitioning from the world of the living to the spiritual world [7]. Individuals from this region believe that the transition should be facilitated by surviving relatives through funeral and burial rituals. Communities perceive that if the deceased does not attain the elevated rank of ancestral spirit, their spirit may return and punish the living relatives [6]. Hence, several unique funeral and burial practices that more often involve excessive contact with a corpse are often performed to appease the dead. In its global alert and response report of WHO concurred with this assertion by suggesting that nearly 60% of all Ebola cases in Guinea between 2013 and 2014 were a result of traditional burial practices [8]. Cognizant of this, it is essential to gain a better and more comprehensive understanding of the impact of funeral and burial practices during EVD outbreaks to develop feasible intervention and management strategies. Among the several tools and techniques that can be used to explore this phenomenon is mathematical modeling.

Mathematical modelling, as a powerful tool in quantifying the complex and numerous factors, has been widely developed to explore the transmission of EVD [9, 10, 11]. Mathematical

54 modeling is described as the conversion of a real problem in a mathematical form. Modeling,
55 therefore, involves the formulation of the real-life situations or converting the problems in
56 mathematical explanations to a real or believable situation (see for example [12, 13].

57 Mathematical models with classical-order differential equations have especially received
58 great attention (see, [14, 15, 16, 17, 18, 19, 20, 21, 22]) and have widely been used in disease
59 modeling. However, recent studies suggest that models with integer-order derivatives do not
60 adequately capture hereditary properties, long-range interactions, and memory effects that
61 exist in biological systems which have many applications in the fields of science, compared to
62 fractional-order derivatives [23, 24, 25, 26, 27]. It is documented literature that models that
63 utilize fractional-order derivatives capture hereditary properties, memory effects, and enlarge
64 the region of stability [27]. Previous studies suggest that without memory effects evolution
65 and control of diseases in communities can not be considered [28]. In particular, whenever
66 the disease spreads in societies, humans gain experience which influence in control of spread
67 disease in the community [27, 29]. Additionally, cell membrane of living organisms contain
68 some fractional order-electrical conductance which are classified in groups of fractional order
69 models [23, 28].

70 Recently, Ivan et al. [30], Muhammad et al. [31], Dokuyucua and Dutta [32], Farman et
71 al.[33], Singh[34] and Pan et al. [35] used the fractional-order derivatives to study the effect
72 of memory on EVD dynamics. Dokuyucua and Dutta [32] utilised Caputo fractional-order
73 differential equations without singular kernel to explore the effects of memory on spread of
74 Ebola in Africa. Among several other outcomes, they found out that their model solution-
75 s were in agreement with reality. Muhammad et al. [31] proposed and studied a nonlinear
76 time-fractional mathematical model of the Ebola Virus to understand the outbreak of dis-
77 ease in the community. Their model analysis included both Caputo and Atangana Baleanu
78 fractional derivative operators to solve the solution of the system of fractional differential e-
79 quations. One of the key findings from their work was that fractional-order derivative showed
80 significant changes and memory effects compared to classical-order derivatives. Farman et
81 al. [33] studied a nonlinear fractional order Ebola virus mathematical model to explore the
82 effects control strategies on the spread of disease in the population. They used Laplace with
83 Adomian Decomposition to solved the fractional differential systems. Their results revealed
84 that, as the order of derivative decreased, the disease died out in the population. Area et al.
85 [30] used both classical and fractional order Ebola epidemic model to fit the real data of Ebola
86 cases reported in Guinea, Liberia and Sierra Leone. In numerical simulations, they found that

87 the fractional-order model gave a better prediction of the disease compared to classical order
88 derivatives. Mathematical studies of fractional order differential equations in disease modeling
89 are also found in [28, 36, 37, 38, 39, 40, 41, 42] and the references therein.

90 Mathematical modelling, as a powerful tool in quantifying the complex and numerous
91 factors, has widely been developed to explore the transmission dynamics of EVD [9, 10, 11].
92 One of the emerging areas in biological research is to understand the role of memory effects on
93 the short and long-term dynamics of infectious diseases. Thus, in this study a mathematical
94 model for EVD based on Fractional Calculus is proposed and analyzed. Although this is not the
95 first study to incorporate Fractional Calculus in analyzing EVD transmission (see, for example
96 [30, 34, 43], the proposed model is unique from those in literature in that it also incorporates
97 the direct and indirect disease transmission rates, and effects of cultural beliefs and educational
98 campaigns on funeral and burial practices. Here, EVD transmission rate is being modeled by
99 the mass action incidence which is appropriate when the population is not too large [44]. One
100 of the most commonly performed funeral rituals, which significantly contributes to the spread
101 of Ebola, is the washing and cleaning of dead bodies. Another burial ritual involves relatives
102 of the deceased washing their hands in a common bowl after which they touch the face of
103 the deceased in what is perceived as a ‘love touch’ that cements unity between the living and
104 ancestral spirits [45]. We assume that the transmission rate of EVD is dependent on the size of
105 the population attending funerals and the burial practices which implies that the contact rate
106 is an increasing function of the population. The mass action incidence is density- dependent
107 since contact rate per infective is proportional to the density of infectious hosts.

108 Motivated by the above-mentioned works, we derive a fractional-order model for EVD
109 based on the Caputo derivative. The choice of Caputo derivative is also aided by the fact
110 that the Caputo derivative for a given function which is constant is zero. Thus, the Caputo
111 operator computes an ordinary differential equation, followed by a fractional integral to obtain
112 the desired order of fractional derivative [37, 46, 47]. Most importantly, the Caputo fractional
113 derivative allows the use of local initial conditions to be included in the derivation of the model
114 [29, 34, 47, 48].

115 In Section 2, we present the preliminaries on the Caputo fractional calculus. The proposed
116 model and analytical results are presented in Section 3. In Section 4, the numerical simulations
117 are done to verify the theoretical results presented in the study. Finally, a concluding remark
118 rounds up the paper.

119 **2 Preliminary Results**

120 The basic idea of fractional order derivative was first initiated by Riemann and Liouville, and
121 another by Caputo which is based on the exponential kernel. The main advantage of Caputo
122 fractional order derivative over Riemann-Liouville fractional operator is that: Caputo fractional
123 order derivative provides standard initial conditions which have clear physical interpretation of
124 the problem. Besides, Caputo fractional order derivative is bounded, meaning that the deriva-
125 tive of any constant function is zero. Motivated by the benefits of Caputo fractional operator
126 over the other operators, the proposed model in this study is based on the Caputo fractional
127 derivatives which is an important tool for describing the memory and heredity properties.

128 **2.1 Mathematical concepts of fractional order**

129 In this section we start with mathematical concepts of of Caputo fractional order derivatives
130 which will be used in analysis of proposed Ebola model (see,[28, 49]). The details can be
131 obtained in Appendix A.

132 **3 Description of Model and Analytical Results**

133 Motivated by the works in [9, 10, 11, 30, 43, 34], we are concerned with the impact of ed-
134 ucational campaigns on funeral and burial practices. We subdivide the total population of
135 humans $N(t)$ into categories of: susceptible population unaware of the disease fighting means
136 $S(t)$, susceptible population aware of the disease fighting means $E(t)$; infected individuals who
137 are displaying clinical signs of the disease and are infectious $I(t)$, individuals who have recov-
138 ered from infection $R(t)$, and the deceased population $D(t)$. Let $P(t)$ denote the pathogen
139 population in the environment.

140 The EVD transmission rate is modeled by the mass action incidence which is appropriate
141 when $N(t)$ is not too large [44]. We assume that the transmission rate is dependent on the
142 size of the population which implies that the contact rate is an increasing function of the
143 population. The mass action incidence is density- dependent since the contact rate per infective
144 is proportional to the density of the infectious host.

145 The proposed fractional-order derivatives EVD model is given by:

$$\left. \begin{aligned}
D_{t_0}^\alpha S(t) &= \Lambda - (\beta_1 I(t) + \beta_2 D(t) + \lambda P(t))S(t) + \phi E(t) - (\mu + \psi)S(t), \\
D_{t_0}^\alpha E(t) &= \psi S(t) - \gamma(\beta_1 I(t) + \beta_2 D(t) + \lambda P(t))E(t) - (\phi + \mu)E(t), \\
D_{t_0}^\alpha I(t) &= (\beta_1 I(t) + \beta_2 D(t) + \lambda P(t))(S(t) + \gamma E(t)) - (\mu + \sigma + \delta)I(t), \\
D_{t_0}^\alpha R(t) &= \sigma I(t) - \mu R(t), \\
D_{t_0}^\alpha D(t) &= (\mu + \delta)I(t) - \epsilon D(t), \\
D_{t_0}^\alpha P(t) &= \rho I(t) + \theta D(t) - (\tau + \eta)P(t),
\end{aligned} \right\} \quad (1)$$

148 where $D_{t_0}^\alpha$ denotes the Caputo-fractional calculus and α with $0 < \alpha \leq 1$ is the fractional order.

149 The model flow diagram is depicted in Figure 1.

150 Additional biological and epidemiological assumptions that govern the model (1) are::

151 (i) Model (1) exhibits some time dimension problems between left-and right-hand sides of
152 the equations. On the left, the dimension is $(time)^{-\alpha}$, whereas on the right-hand side
153 the dimension is $(time)^{-1}$. To balance the model, the corrected system corresponding to
154 model (1) is as follows:

$$\left. \begin{aligned}
D_{t_0}^\alpha S(t) &= \Lambda^\alpha - (\beta_1^\alpha I(t) + \beta_2^\alpha D(t) + \lambda^\alpha P(t))S(t) + \phi^\alpha E(t) - (\mu^\alpha + \psi^\alpha)S(t), \\
D_{t_0}^\alpha E(t) &= \psi^\alpha S(t) - \gamma^\alpha(\beta_1^\alpha I(t) + \beta_2^\alpha D(t) + \lambda^\alpha P)E(t) - (\phi^\alpha + \mu^\alpha)E(t), \\
D_{t_0}^\alpha I(t) &= (\beta_1^\alpha I(t) + \beta_2^\alpha D(t) + \lambda^\alpha P(t))(S(t) + \gamma^\alpha E(t)) - (\mu^\alpha + \sigma^\alpha + \delta^\alpha)I(t), \\
D_{t_0}^\alpha R(t) &= \sigma^\alpha I(t) - \mu^\alpha R(t), \\
D_{t_0}^\alpha D(t) &= (\mu^\alpha + \delta^\alpha)I(t) - \epsilon^\alpha D(t), \\
D_{t_0}^\alpha P(t) &= \rho^\alpha I(t) + \theta^\alpha D(t) - (\tau^\alpha + \eta^\alpha)P(t),
\end{aligned} \right\} \quad (2)$$

156 (ii) All new recruits are assumed to be susceptible and unaware of the disease and recruited
157 at the rate Λ . Natural mortality occurs at the rate μ . Meanwhile, the susceptible
158 populations are educated at the rate ψ per-day and some educated populations can stop
159 following the preventive measures at the rate ϕ . There is evidence in [50, 51] that Ebola
160 outbreak can last for more than two years which allows the demographic process to take
161 place. Therefore, we have included vital dynamics in our model since the 2014 Ebola
162 outbreak in Guinea.

163 (iii) Susceptible unaware individuals become aware of the infection through educational cam-
164 paigns at the rate ψ . Due to memory fading and/or carelessness, susceptible aware
165 individuals become unaware individuals at the rate ϕ :

- 166 (iv) Susceptible individuals are assumed to acquire the infection either directly (through con-
 167 tact with either infectious individuals or deceased EVD patients) or, indirectly through
 168 contaminated environment. Model parameters β_1 , β_2 and λ account for disease transmis-
 169 sion when susceptible individuals come into contact with infectious individuals, deceased
 170 patients and the environment respectively. Susceptible aware individuals are assumed
 171 to have reduced chances of contracting the disease, modeled by $0 < \gamma < 1$, where γ is
 172 the disease modification factor that accounts for the impact of educational campaigns on
 173 disease transmission.
- 174 (v) Infected individuals either recover from infection permanently (at the rate σ) or, succumb
 175 to disease-related death at the rate δ . The deceased individual are buried after ϵ^{-1} days.
 176 Infectious and deceased EVD patients contaminate the environment at the rates ρ and θ ,
 177 respectively. The population of pathogens in the environment decreases due to natural
 178 decay (at the rate τ) or decontamination (at the rate η).

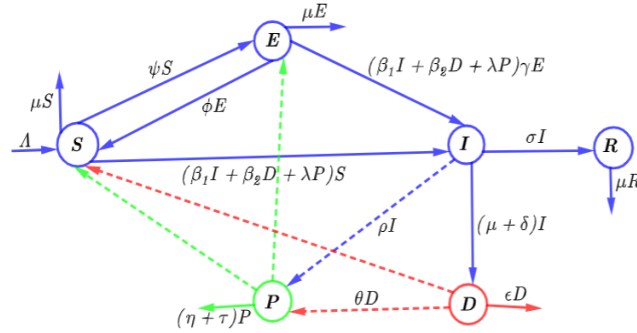


Figure 1: Flow chart for Ebola virus disease

179 3.1 Non-negativity and boundedness of model solutions

180 Since model (2) investigate human population, it is important to demonstrate that all model
 181 solutions are bounded and positive for all $t \geq 0$. From the computations presented in Appendix
 182 B we obtained the following results.

183 **Theorem 3.1.** *Model (2) has unique and non-negative solutions which turn into region Γ_+ as*

184 $t \rightarrow \infty$, where Γ_+ is defined by: $\Gamma_+ = \left\{ (S(t), E(t), I(t), R(t), D(t), P(t)) \in \mathbb{R}_+^6; S(t) + E(t) + \right.$
 185 $I(t) + R(t) + D(t) + P(t) = N = \frac{\Lambda^\alpha}{\mu^\alpha}, D = \frac{(\mu^\alpha + \delta^\alpha) \Lambda^\alpha}{\mu^\alpha \epsilon^\alpha}, P = \frac{\epsilon^\alpha \rho^\alpha \Lambda^\alpha + \theta^\alpha (\mu^\alpha + \delta^\alpha) \Lambda^\alpha}{\mu^\alpha \epsilon^\alpha (\tau^\alpha + \eta^\alpha)} \left. \right\}$

186 3.2 The Basic Reproduction Number

187 In this section, we study the basic reproduction number and the existence of a disease-free equi-
 188 librium and an endemic equilibrium of the model (2). The model (2) always has a disease-free
 189 equilibrium $\mathcal{E}^0 = (S^0, E^0, I^0, D^0, P^0, R^0) = (S^0, E^0, 0, 0, 0, 0)$, with $S^0 = \frac{\Lambda^\alpha(\phi^\alpha + \mu^\alpha)}{\mu^\alpha(\mu^\alpha + \phi^\alpha + \psi^\alpha)}$,
 190 $E^0 = \frac{\Lambda^\alpha\psi^\alpha}{\mu^\alpha(\mu^\alpha + \phi^\alpha + \psi^\alpha)}$, and $S^0 + \gamma^\alpha E^0 = \frac{\Lambda^\alpha(\phi^\alpha + \mu^\alpha + \gamma^\alpha\psi^\alpha)}{\mu^\alpha(\mu^\alpha + \phi^\alpha + \psi^\alpha)}$. By means of the next gen-
 191 eration matrix (see, for example, van den Driessche and Watmough [18], one obtains the basic
 192 reproduction number of the model (2) as follows:

$$\begin{aligned} \mathcal{R}_0 = & \frac{(S^0 + \gamma^\alpha E^0)\beta_1^\alpha}{(\mu^\alpha + \sigma^\alpha + \delta^\alpha)} + \frac{(S^0 + \gamma^\alpha E^0)(\mu^\alpha + \delta^\alpha)\beta_2^\alpha}{\epsilon^\alpha(\mu^\alpha + \sigma^\alpha + \delta^\alpha)} + \frac{(S^0 + \gamma^\alpha E^0)\theta^\alpha(\mu^\alpha + \delta^\alpha)\lambda^\alpha}{\epsilon^\alpha(\tau^\alpha + \eta^\alpha)(\mu^\alpha + \sigma^\alpha + \delta^\alpha)} \\ & + \frac{(S^0 + \gamma^\alpha E^0)\rho^\alpha\lambda^\alpha}{(\tau^\alpha + \eta^\alpha)(\mu^\alpha + \sigma^\alpha + \delta^\alpha)} \end{aligned} \quad (3)$$

194 Biologically, the basic reproduction number \mathcal{R}_0 represents the average number of new or
 195 secondary EVD infections caused by the introduction of an infectious individual into a to-
 196 tally susceptible population. It follows that model (2) has a disease-free equilibrium point
 197 $\mathcal{E}^0 = (S^0, E^0, I^0, D^0, P^0, R^0)$ which exists whenever $\mathcal{R}_0 < 1$ and it provides a criterion for the
 198 extinction of the disease. In addition to the disease-free equilibrium \mathcal{E}^0 , the model (2) has a
 199 unique endemic equilibrium point $\mathcal{E}^* = (S^*, E^*, I^*, D^*, P^*, R^*)$, which exists whenever $\mathcal{R}_0 > 1$,
 200 the EVD infection persists, where:

$$S^* = \frac{\Lambda^\alpha[\gamma^\alpha(\beta_1^\alpha I^* + \beta_2^\alpha D^* + \lambda^\alpha P^*) + (\mu^\alpha + \phi^\alpha)]}{n_1 n_2 - \phi^\alpha \psi^\alpha}, \quad (4)$$

$$E^* = \frac{\Lambda^\alpha \psi^\alpha}{n_1 n_2 - \phi^\alpha \psi^\alpha}, \quad (5)$$

204 with $n_1 = [(\beta_1^\alpha I^* + \beta_2^\alpha D^* + \lambda^\alpha P^*) + (\mu^\alpha + \psi^\alpha)]$ and $n_2 = [\gamma^\alpha(\beta_1^\alpha I^* + \beta_2^\alpha D^* + \lambda^\alpha P^*) + (\mu^\alpha + \phi^\alpha)]$

$$\begin{aligned} D^* &= \frac{(\mu^\alpha + \delta^\alpha)I^*}{\epsilon^\alpha}, & R^* &= \frac{\rho^\alpha I^*}{\mu^\alpha}, & \text{and} \\ P^* &= \frac{\rho^\alpha I^*}{(\tau^\alpha + \eta^\alpha)} + \frac{\theta^\alpha(\mu^\alpha + \delta^\alpha)I^*}{\epsilon^\alpha(\tau^\alpha + \eta^\alpha)}. \end{aligned} \quad (6)$$

206 Substituting equation (6) into the third equation in (2), gives:

$$\begin{aligned} & \beta_1^\alpha I^*(S^* + \gamma^\alpha E^*) + \frac{\beta_2^\alpha(\mu^\alpha + \delta^\alpha)I^*(S^* + \gamma^\alpha E^*)}{\epsilon^\alpha} + \frac{\lambda^\alpha \rho^\alpha I^*(S^* + \gamma^\alpha E^*)}{(\tau^\alpha + \eta^\alpha)} \\ & + \frac{\lambda^\alpha \theta^\alpha(\mu^\alpha + \delta^\alpha)I^*(S^* + \gamma^\alpha E^*)}{\epsilon^\alpha(\tau^\alpha + \eta^\alpha)} - (\mu^\alpha + \sigma^\alpha + \delta^\alpha)I^* = 0. \end{aligned} \quad (7)$$

208 From (31), we have:

$$\begin{aligned}
& \left(\frac{\beta_1^\alpha I^*(S^* + \gamma^\alpha E^*)}{(\mu^\alpha + \sigma^\alpha + \delta^\alpha)} + \frac{\beta_2^\alpha (\mu^\alpha + \delta^\alpha) I^*(S^* + \gamma^\alpha E^*)}{\epsilon^\alpha (\mu^\alpha + \sigma^\alpha + \delta^\alpha)} + \frac{\lambda^\alpha \rho^\alpha I^*(S^* + \gamma^\alpha E^*)}{(\tau^\alpha + \eta^\alpha) (\mu^\alpha + \sigma^\alpha + \delta^\alpha)} \right. \\
& \left. + \frac{\lambda^\alpha \theta^\alpha (\mu^\alpha + \delta^\alpha) I^*(S^* + \gamma^\alpha E^*)}{\epsilon^\alpha (\tau^\alpha + \eta^\alpha) (\mu^\alpha + \sigma^\alpha + \delta^\alpha)} - 1 \right) \times (\mu^\alpha + \sigma^\alpha + \delta^\alpha) I^* = 0.
\end{aligned}$$

210 It follows that:

$$211 \quad I^* = 0, \quad \text{or}$$

212

$$213 \quad (S^* + \gamma^\alpha E^*) = \frac{\epsilon^\alpha (\tau^\alpha + \eta^\alpha) (\mu^\alpha + \sigma^\alpha + \delta^\alpha)}{r}, \quad (8)$$

214 with $r = \beta_1^\alpha \epsilon^\alpha (\tau^\alpha + \eta^\alpha) + \beta_2^\alpha \eta^\alpha (\mu^\alpha + \delta^\alpha) + \lambda^\alpha \epsilon^\alpha \rho^\alpha + \theta^\alpha \lambda^\alpha (\mu^\alpha + \delta^\alpha)$. Substituting the value of

215 S^* and E^* into (32), yields:

$$216 \quad g(I^*) = A(I^*)^2 + BI^* + C, \quad (9)$$

217 where:

$$\begin{aligned}
A &= \epsilon^\alpha (\tau^\alpha + \eta^\alpha) (\mu^\alpha + \sigma^\alpha + \delta^\alpha) \gamma^\alpha \lambda^{2\alpha} \times \left[\frac{\rho^\alpha}{(\tau^\alpha + \eta^\alpha)} + \frac{\theta^\alpha (\mu^\alpha + \delta^\alpha)}{\epsilon^\alpha (\tau^\alpha + \eta^\alpha)} \right]^2 \\
&+ \epsilon^\alpha (\tau^\alpha + \eta^\alpha) (\mu^\alpha + \sigma^\alpha + \delta^\alpha) \gamma^\alpha \beta_1^{\alpha} + \frac{(\tau^\alpha + \eta^\alpha) (\mu^\alpha + \sigma^\alpha + \delta^\alpha) \gamma^\alpha \beta_2^{2\alpha} (\mu^\alpha + \delta^\alpha)^2}{\epsilon^\alpha} \\
&+ 2(\tau^\alpha + \eta^\alpha) (\mu^\alpha + \sigma^\alpha + \delta^\alpha) (\mu^\alpha + \delta^\alpha) \gamma^\alpha \beta_1^\alpha \beta_2^\alpha + 2\gamma^\alpha \beta_1^\alpha \lambda^\alpha (\mu^\alpha + \sigma^\alpha + \delta^\alpha) (\rho^\alpha \epsilon^\alpha + \theta^\alpha (\mu^\alpha \\
&+ \delta^\alpha)) + 2\gamma^\alpha \beta_2^\alpha \lambda^\alpha (\mu^\alpha + \sigma^\alpha + \delta^\alpha) (\mu^\alpha + \delta^\alpha) \times \left(\rho^\alpha + \frac{\theta^\alpha (\mu^\alpha + \delta^\alpha)}{\epsilon^\alpha} \right),
\end{aligned}$$

$$\begin{aligned}
B &= \left[\gamma^\alpha \mu^\alpha + (\mu^\alpha + \phi^\alpha + \gamma^\alpha \psi^\alpha) - \frac{M}{\epsilon^\alpha (\tau^\alpha + \eta^\alpha) (\mu^\alpha + \sigma^\alpha + \delta^\alpha)} \right] \\
&\times (\mu^\alpha + \sigma^\alpha + \delta^\alpha) [\beta_1^\alpha \epsilon^\alpha (\tau^\alpha + \eta^\alpha) + \beta_2^\alpha (\tau^\alpha + \eta^\alpha) (\mu^\alpha + \delta^\alpha) + \lambda^\alpha \epsilon^\alpha \rho^\alpha + \theta^\alpha \lambda^\alpha (\mu^\alpha + \delta^\alpha)],
\end{aligned}$$

$$218 \quad C = \epsilon^\alpha \mu^\alpha (\tau^\alpha + \eta^\alpha) (\mu^\alpha + \sigma^\alpha + \delta^\alpha) (\mu^\alpha + \phi^\alpha + \psi^\alpha) [1 - \mathcal{R}_0], \text{ where,}$$

$$219 \quad M = \gamma^\alpha \Lambda^\alpha (\beta_1^\alpha \epsilon^\alpha (\tau^\alpha + \eta^\alpha) + \beta_2^\alpha (\tau^\alpha + \eta^\alpha) (\mu^\alpha + \delta^\alpha) + \lambda^\alpha \epsilon^\alpha \rho^\alpha + \theta^\alpha \lambda^\alpha (\mu^\alpha + \delta^\alpha)).$$

219 Using the fact that all parameters in the model (2) are positive for $t \geq 0$, it follows from

220 Equation (9) that $A > 0$. Furthermore, $C > 0$ when $\mathcal{R}_0 < 1$. Therefore, the number of

221 possible positive real roots of the polynomial (9) hinges on the signs of B and C . By applying
 222 the Descartes rule of signs on the polynomial (9) $g(I^*) = 0$, given in (9), we list the various
 223 possibilities for the roots of $g(I^*)$ in Table 1:

Table 1: Number of various possibilities for the roots of $g(I^*)$ for $\mathcal{R}_0 < 1$ and $\mathcal{R}_0 > 1$.

Case	A	B	C	\mathcal{R}_0	No. of sign changes	No. of various possibilities for the roots
1	+	+	+	$\mathcal{R}_0 < 1$	0	0
2	+	+	-	$\mathcal{R}_0 > 1$	1	1
3	+	-	+	$\mathcal{R}_0 < 1$	2	0,2
4	+	-	-	$\mathcal{R}_0 > 1$	1	1

224 Based on the various possibilities in Table 1, we have the following results:

225 **Theorem 3.2.** *The model (2) admits that:*

- 226 (i) *a unique endemic equilibrium \mathcal{E}^* if $\mathcal{R}_0 > 1$ and Cases 2 and 4 are satisfied,*
 227 (ii) *more than one endemic equilibrium if $\mathcal{R}_0 < 1$ part of Case 3 holds,*
 228 (iii) *no endemic equilibrium if $\mathcal{R}_0 < 1$, and Cases 1 and part of Case 3 are satisfied.*

229 3.3 Global Stability

230 In this section, we are concerned with the global stability of the disease-free equilibrium $\mathcal{E}^0 =$
 231 $(S^0, E^0, 0, 0, 0, 0)$ and the endemic equilibrium $\mathcal{E}^* = (S^*, E^*, I^*, D^*, P^*, R^*)$ of the model (2).
 232 To investigate the global stability of the model steady states we will construct appropriate
 233 Lyapunov functionals. Since the recovered/removed population does not contribute to the
 234 generation of secondary infections one can ignore that fourth equation of model (2) when
 235 examining the global stability and consider the following reduced system:

$$\left. \begin{aligned}
 D_{t_0}^\alpha S(t) &= \Lambda^\alpha - (\beta_1^\alpha I(t) + \beta_2^\alpha D(t) + \lambda^\alpha P(t))S(t) + \phi^\alpha E(t) - m_1 S(t), \\
 D_{t_0}^\alpha E(t) &= \psi^\alpha S(t) - \gamma^\alpha (\beta_1^\alpha I(t) + \beta_2^\alpha D(t) + \lambda^\alpha P)E(t) - m_2 E(t), \\
 D_{t_0}^\alpha I(t) &= [(\beta_1^\alpha I(t) + \beta_2^\alpha D(t) + \lambda^\alpha P(t))S(t) + \gamma^\alpha (\beta_1^\alpha I(t) + \beta_2^\alpha D(t) + \lambda^\alpha P)E(t)] \\
 &\quad - m_3 I(t), \\
 D_{t_0}^\alpha D(t) &= m_4 I(t) - \epsilon^\alpha D(t), \\
 D_{t_0}^\alpha P(t) &= \rho^\alpha I(t) + \theta^\alpha D(t) - m_5 P(t),
 \end{aligned} \right\} (10)$$

237 with $m_1 = (\mu^\alpha + \psi^\alpha)$, $m_2 = (\phi^\alpha + \mu^\alpha)$, $m_3 = (\mu^\alpha + \sigma^\alpha + \delta^\alpha)$, $m_4 = (\mu^\alpha + \delta^\alpha)$, and $m_5 = (\tau^\alpha + \eta^\alpha)$.
 238 To investigate the global stability of the disease-free equilibrium point \mathcal{E}^0 and the endemic
 239 equilibrium \mathcal{E}^* of model (10), we utilize the Lyapunov function whose origin is ecology but
 240 was extended to epidemiology models and then effectively applied to a variety of compartment
 241 models (see for example [56]).

242 We begin by introducing the following definition of positive definite function (see, [57]) that
 243 we use to develop the Lyapunov's function.

244 **Definition 1. (Positive definite function [57])** Let $\mathcal{V}(t) : \mathbb{R}^n \rightarrow \mathbb{R}$ be a continuously
 245 differentiable real valued function. Then $\mathcal{V}(t)$ is said to be positive definite function if:

- 246 1. $\mathcal{V}(t^0) = 0$, and:
- 247 2. $\mathcal{V}(t) > 0$ for all $t \neq t^0$

248 **Theorem 3.3.** (Fractional La-Salle invariance principle [28, 49]). Let $x^* \in \Gamma \subset \mathbb{R}^n$ be
 249 an equilibrium point for the non-autonomous fractional order system $D_{t_0}^\alpha = f(t, x)$. Let $L : [0, \infty) \times \Gamma \rightarrow \mathbb{R}$ be a continuously differentiable function such that:

$$251 \quad \mathcal{M}_1(x) \leq L(t, x(t)) \leq \mathcal{M}_2(x)$$

252 and:

$$253 \quad D_{t_0}^\alpha L(t, x(t)) \leq -\mathcal{M}_3(x),$$

254 for all $\alpha \in (0, 1)$ and all $x \in \Gamma$, where $\mathcal{M}_1(x)$, $\mathcal{M}_2(x)$ and $\mathcal{M}_3(x)$ are continuous positive
 255 definite functions on Γ . Then the equilibrium point x^* is uniformly asymptotically stable.

256 Now using Theorem (3.3) we will show that the disease-free equilibrium \mathcal{E}^0 and the endemic
 257 equilibrium point \mathcal{E}^* of system (10) are globally asymptotically stable

258 **Theorem 3.4.** For $\alpha \in (0, 1]$, the disease-free equilibrium \mathcal{E}^0 of system (10) is globally asymp-
 259 totically stable whenever $\mathcal{R}_0 \leq 1$.

260 *Proof.* Consider the following appropriate Lyapunov function:

$$261 \quad \mathcal{V}(t) = \left(\frac{\beta_1^\alpha}{m_3} + \frac{\beta_2^\alpha m_4}{\epsilon^\alpha m_3} + \frac{\theta^\alpha \lambda^\alpha m_4}{\epsilon^\alpha m_5 m_3} + \frac{\lambda^\alpha \rho^\alpha}{m_5 m_3} \right) I(t) + \left(\frac{\beta_2^\alpha}{\epsilon^\alpha} + \frac{\theta^\alpha \lambda^\alpha}{\epsilon^\alpha m_5} \right) D(t) + \frac{\lambda^\alpha}{m_5} P(t).$$

262 Then the time fractional order derivative of $\mathcal{V}(t)$ along solutions of model (10):

$$D_{t_0}^\alpha \mathcal{V}(t) = \left(\frac{\beta_1^\alpha}{m_3} + \frac{\beta_2^\alpha m_4}{\epsilon^\alpha m_3} + \frac{\theta^\alpha \lambda^\alpha m_4}{\epsilon^\alpha m_5 m_3} + \frac{\lambda^\alpha \rho^\alpha}{m_5 m_3} \right) \times \left(\beta_1^\alpha I(t) + \beta_2^\alpha D(t) + \lambda^\alpha P(t) \right)$$

$$\begin{aligned}
& \times \left(S(t) + \gamma^\alpha E(t) \right) - \left(\beta_1^\alpha I(t) + \beta_2^\alpha D(t) + \lambda^\alpha P(t) \right) \\
& = \left[\left(\frac{\beta_1^\alpha}{m_3} + \frac{\beta_2^\alpha m_4}{\epsilon^\alpha m_3} + \frac{\theta^\alpha \lambda^\alpha m_4}{\epsilon^\alpha m_5 m_3} + \frac{\lambda^\alpha \rho^\alpha}{m_5 m_3} \right) \times \left(S(t) + \gamma^\alpha E(t) \right) - 1 \right] \\
& \quad \times \left[\beta_1^\alpha I(t) + \beta_2^\alpha D(t) + \lambda^\alpha P(t) \right].
\end{aligned}$$

263

264 Since $S^0 \leq S(t), E^0 \leq E(t), \left(S^0 + \gamma^\alpha E^0 = \frac{\Lambda^\alpha(\phi^\alpha + \mu^\alpha + \gamma^\alpha \psi^\alpha)}{\mu^\alpha(\mu^\alpha + \phi^\alpha + \psi^\alpha)} \right)$ for $t \geq 0$ we have:

$$\begin{aligned}
D_{t_0}^\alpha \mathcal{V}(t) & \leq \left[\left(\frac{\beta_1^\alpha}{m_3} + \frac{\beta_2^\alpha m_4}{\epsilon^\alpha m_3} + \frac{\theta^\alpha \lambda^\alpha m_4}{\epsilon^\alpha m_5 m_3} + \frac{\lambda^\alpha \rho^\alpha}{m_5 m_3} \right) \times \left(\frac{\Lambda^\alpha(\phi^\alpha + \mu^\alpha + \gamma^\alpha \psi^\alpha)}{\mu^\alpha(\mu^\alpha + \phi^\alpha + \psi^\alpha)} \right) - 1 \right] \\
& \quad \times \left[\beta_1^\alpha I(t) + \beta_2^\alpha D(t) + \lambda^\alpha P(t) \right] \\
& = \left[\mathcal{R}_0 - 1 \right] \left[\beta_1^\alpha I(t) + \beta_2^\alpha D(t) + \lambda^\alpha P(t) \right].
\end{aligned} \tag{11}$$

265

266 Therefore, $D_{t_0}^\alpha \mathcal{V}(t) < 0$ holds if $\mathcal{R}_0 < 1$. Furthermore if $\mathcal{R}_0 = 1$, $D_{t_0}^\alpha \mathcal{V}(t) = 0$ if and only
267 if $S(t) = S^0, E(t) = E^0, I(t) = D(t) = P(t) = 0$. Thus, the largest compact invariant
268 set in $U_1 = \{(S^0, E^0, 0, 0, 0) \in \Gamma : D_{t_0}^\alpha \mathcal{V}(t) = 0\}$ is a singleton set containing the disease-free
269 equilibrium \mathcal{E}^0 . Therefore, by Theorem (3.3), we conclude that the disease-free equilibrium is
270 globally asymptotically stable in Γ . \square

271 Next, we investigate the global stability of the endemic equilibrium point \mathcal{E}^* of model (10)
272 when $\mathcal{R}_0 > 1$.

273 **Theorem 3.5.** For $\alpha \in (0, 1]$, whenever $\mathcal{R}_0 > 1$, then model (10) has a globally asymptotically
274 stable endemic equilibrium point \mathcal{E}^* .

275 *Proof.* Let us consider the following appropriate Lyapunov function:

$$\begin{aligned}
\mathcal{W}(t) & = \left\{ S(t) - S^* - S^* \ln \left(\frac{S(t)}{S^*} \right) \right\} + \left\{ E(t) - E^* - E^* \ln \left(\frac{E(t)}{E^*} \right) \right\} \\
& \quad + \left\{ I(t) - I^* - I^* \ln \left(\frac{I(t)}{I^*} \right) \right\} + \frac{[\beta_2^\alpha D^* (\rho^\alpha I^* + \theta^\alpha D^*) + \lambda^\alpha P^* \theta^\alpha D^*] (S^* + \gamma^\alpha E^*)}{m_4 I^* [\rho^\alpha I^* + \theta^\alpha D^*]} \\
& \quad \times \left\{ D(t) - D^* - D^* \ln \left(\frac{D(t)}{D^*} \right) \right\} + \frac{\lambda^\alpha P^* (S^* + \gamma^\alpha E^*)}{[\rho^\alpha I^* + \theta^\alpha D^*]} \\
& \quad \times \left\{ P(t) - P^* - P^* \ln \left(\frac{P(t)}{P^*} \right) \right\}
\end{aligned} \tag{12}$$

276

277

278 The time fractional order derivatives of $\mathcal{W}(t)$ are given by:

$$\begin{aligned}
D_{t_0}^\alpha \mathcal{W}(t) &= \left(1 - \frac{S^*}{S(t)}\right) D_{t_0}^\alpha S(t) + \left(1 - \frac{E^*}{E(t)}\right) D_{t_0}^\alpha E(t) + \left(1 - \frac{I^*}{I(t)}\right) D_{t_0}^\alpha I(t) \\
&\quad + \frac{[\beta_2^\alpha D^*(\rho^\alpha I^* + \theta^\alpha D^*) + \lambda^\alpha P^* \theta^\alpha D^*]}{m_4 I^* [\rho^\alpha I^* + \theta^\alpha D^*]} \times (S^* + \gamma^\alpha E^*) \left(1 - \frac{D^*}{D(t)}\right) D_{t_0}^\alpha D(t) \\
&\quad + \frac{\lambda^\alpha P^* (S^* + \gamma^\alpha E^*)}{[\rho^\alpha I^* + \theta^\alpha D^*]} \left(1 - \frac{P^*}{P(t)}\right) D_{t_0}^\alpha P(t). \tag{13}
\end{aligned}$$

280 Substituting the appropriate derivatives according to equations (10), we have:

$$\begin{aligned}
D_{t_0}^\alpha \mathcal{W}(t) &= \left\{1 - \frac{S^*}{S(t)}\right\} \left\{ \psi^\alpha S(t) - \gamma^\alpha (\beta_1^\alpha I(t) + \beta_2^\alpha D(t) + \lambda^\alpha P) E(t) - (\phi^\alpha + \mu^\alpha) E(t) \right\} \\
&\quad + \left\{1 - \frac{E^*}{E(t)}\right\} \left\{ \psi^\alpha S(t) - \phi^\alpha E(t) - \mu^\alpha E - \gamma^\alpha \beta_1^\alpha I(t) E(t) - \gamma^\alpha \beta_2^\alpha D_1(t) E(t) \right\} \\
&\quad + \left\{1 - \frac{I^*}{I(t)}\right\} \left\{ [(\beta_1^\alpha I(t) + \beta_2^\alpha D(t) + \lambda^\alpha P(t)) S(t) + \gamma^\alpha (\beta_1^\alpha I(t) + \beta_2^\alpha D(t) \right. \\
&\quad \left. + \lambda^\alpha P) E(t)] \right. \\
&\quad \left. - (\mu^\alpha + \sigma^\alpha + \delta^\alpha) I(t) \right\} + \frac{[\beta_2^\alpha D^*(\rho^\alpha I^* + \theta^\alpha D^*) + \lambda^\alpha P^* \theta^\alpha D^*] (S^* + \gamma^\alpha E^*)}{m_4 I^* [\rho^\alpha I^* + \theta^\alpha D^*]} \\
&\quad \times \left\{1 - \frac{D^*}{D(t)}\right\} \left\{ (\mu^\alpha + \delta^\alpha) I(t) - \epsilon^\alpha D(t) \right\} + \frac{\lambda^\alpha P^* (S^* + \gamma^\alpha E^*)}{[\rho^\alpha I^* + \theta^\alpha D^*]} \left\{1 - \frac{P^*}{P(t)}\right\} \\
&\quad \times \left\{ \rho^\alpha I(t) + \theta^\alpha D(t) - (\tau^\alpha + \eta^\alpha) P(t) \right\}. \tag{14}
\end{aligned}$$

283 At endemic equilibrium, we have:

$$\left\{ \begin{array}{l}
\Lambda^\alpha = \beta_1^\alpha I^* S^* + \beta_2^\alpha D^* S^* + \lambda^\alpha P^* S^* + \mu^\alpha S^* + \psi^\alpha S^* - \phi^\alpha E^*, \\
\psi^\alpha S^* = \phi^\alpha E^* + \mu^\alpha E^* + \gamma^\alpha \beta_1^\alpha I^* E(t) + \gamma^\alpha \beta_2^\alpha D^* E^* + \gamma^\alpha \lambda^\alpha P^* E^*, \\
(\mu^\alpha + \sigma^\alpha + \delta^\alpha) I^* = \beta_1^\alpha I^* S^* + \beta_2^\alpha D^* S^* + \lambda^\alpha P^* S^* + \gamma^\alpha \beta_1^\alpha I^* E^* + \gamma^\alpha \beta_2^\alpha D^* E^* \\
\quad + \gamma^\alpha \lambda^\alpha P^* E^*, \\
\epsilon^\alpha D^* = (\mu^\alpha + \delta^\alpha) I^*, \\
(\tau^\alpha + \eta^\alpha) P^* = \rho^\alpha I^* + \theta^\alpha D^*.
\end{array} \right. \tag{15}$$

285 Using the above constants at endemic equilibrium, we have:

$$\begin{aligned}
D_{t_0}^\alpha \mathcal{W}(t) &= (\mu^\alpha + \beta_1^\alpha I^*) S^* \left\{ 2 - \frac{S(t)}{S^*} - \frac{S^*}{S(t)} \right\} + (\mu^\alpha + \gamma^\alpha \beta_1^\alpha I^*) E^* \left\{ 3 - \frac{S(t)}{S^*} \cdot \frac{E^*}{E(t)} \right. \\
&\quad \left. - \frac{S^*}{S(t)} - \frac{E(t)}{E^*} \right\} + \phi^\alpha E^* \left\{ 2 - \frac{S(t)}{S^*} \cdot \frac{E^*}{E(t)} - \frac{S^*}{S(t)} \cdot \frac{E(t)}{E^*} \right\}
\end{aligned}$$

$$\begin{aligned}
& + \frac{\lambda^\alpha P^* S^* \rho^\alpha I^*}{(\rho^\alpha I^* + \theta^\alpha D^*)} \left\{ 3 - \frac{S^*}{S(t)} - \frac{I(t)}{I^*} \cdot \frac{P^*}{P(t)} - \frac{P(t)}{P^*} \cdot \frac{I^*}{I(t)} \cdot \frac{S(t)}{S^*} \right\} \\
& + \frac{\gamma^\alpha \lambda^\alpha P^* E^* \rho^\alpha I^*}{(\rho^\alpha I^* + \theta^\alpha D^*)} \left\{ 4 - \frac{S^*}{S(t)} - \frac{I(t)}{I^*} \cdot \frac{P^*}{P(t)} - \frac{S(t)}{S^*} \cdot \frac{E^*}{E(t)} - \frac{P(t)}{P^*} \cdot \frac{I^*}{I(t)} \cdot \frac{E(t)}{E^*} \right\} \\
& + \frac{\lambda^\alpha P^* S^* \theta^\alpha D^*}{(\rho^\alpha I^* + \theta^\alpha D^*)} \left\{ 4 - \frac{S^*}{S(t)} - \frac{I(t)}{I^*} \cdot \frac{D^*}{D(t)} - \frac{D(t)}{D^*} \cdot \frac{P^*}{P(t)} - \frac{P(t)}{P^*} \cdot \frac{I^*}{I(t)} \cdot \frac{S(t)}{S^*} \right\} \\
& + \frac{\gamma^\alpha \lambda^\alpha P^* E^* \theta^\alpha D^*}{(\rho^\alpha I^* + \theta^\alpha D^*)} \left\{ 5 - \frac{S^*}{S(t)} - \frac{I(t)}{I^*} \cdot \frac{D^*}{D(t)} - \frac{D(t)}{D^*} \cdot \frac{P^*}{P(t)} - \frac{S(t)}{S^*} \cdot \frac{E^*}{E(t)} \right. \\
& \left. - \frac{P(t)}{P^*} \cdot \frac{I^*}{I(t)} \cdot \frac{E(t)}{E^*} \right\} + \beta_2^\alpha S^* D^* \left\{ 3 - \frac{S^*}{S(t)} - \frac{I(t)}{I^*} \cdot \frac{D^*}{D(t)} - \frac{D(t)}{D^*} \cdot \frac{I^*}{I(t)} \cdot \frac{S(t)}{S^*} \right\} \\
& + \gamma^\alpha \beta_2^\alpha E^* D^* \left\{ 4 - \frac{S^*}{S(t)} - \frac{S(t)}{S^*} \cdot \frac{E^*}{E(t)} - \frac{I(t)}{I^*} \cdot \frac{D^*}{D(t)} - \frac{D(t)}{D^*} \cdot \frac{I^*}{I(t)} \cdot \frac{E(t)}{E^*} \right\}. \quad (16)
\end{aligned}$$

286

287 By the property that the arithmetic mean is greater than or equal to the geometric mean:

$$2 \leq \frac{S(t)}{S^*} + \frac{S^*}{S(t)}, \quad 2 \leq \frac{S(t)}{S^*} \cdot \frac{E^*}{E(t)} + \frac{S^*}{S(t)} \cdot \frac{E(t)}{E^*}, \quad 3 \leq \frac{S(t)}{S^*} \cdot \frac{E^*}{E(t)} + \frac{S^*}{S(t)} + \frac{E(t)}{E^*},$$

288

289

$$3 \leq \frac{S^*}{S(t)} + \frac{I(t)}{I^*} \cdot \frac{P^*}{P(t)} + \frac{P(t)}{P^*} \cdot \frac{I^*}{I(t)} \cdot \frac{S(t)}{S^*},$$

290

291

$$4 \leq \frac{S^*}{S(t)} + \frac{I(t)}{I^*} \cdot \frac{P^*}{P(t)} + \frac{S(t)}{S^*} \cdot \frac{E^*}{E(t)} + \frac{P(t)}{P^*} \cdot \frac{I^*}{I(t)} \cdot \frac{E(t)}{E^*},$$

292

293

$$4 \leq \frac{S^*}{S(t)} + \frac{I(t)}{I^*} \cdot \frac{D^*}{D(t)} + \frac{D(t)}{D^*} \cdot \frac{P^*}{P(t)} + \frac{P(t)}{P^*} \cdot \frac{I^*}{I(t)} \cdot \frac{S(t)}{S^*},$$

294

295

$$5 \leq \frac{S^*}{S(t)} + \frac{I(t)}{I^*} \cdot \frac{D^*}{D(t)} + \frac{D(t)}{D^*} \cdot \frac{P^*}{P(t)} + \frac{S(t)}{S^*} \cdot \frac{E^*}{E(t)} + \frac{P(t)}{P^*} \cdot \frac{I^*}{I(t)} \cdot \frac{E(t)}{E^*},$$

296

297

$$3 \leq \frac{S^*}{S(t)} + \frac{I(t)}{I^*} \cdot \frac{D^*}{D(t)} + \frac{D(t)}{D^*} \cdot \frac{I^*}{I(t)} \cdot \frac{S(t)}{S^*},$$

298

299

$$4 \leq \frac{S^*}{S(t)} + \frac{S(t)}{S^*} \cdot \frac{E^*}{E(t)} + \frac{I(t)}{I^*} \cdot \frac{D^*}{D(t)} + \frac{D(t)}{D^*} \cdot \frac{I^*}{I(t)} \cdot \frac{E(t)}{E^*},$$

300

301 for all $S(t) > 0$, $E(t) > 0$, $I(t) > 0$, $D(t) > 0$ and $P(t) > 0$, because the arithmetic mean is

302 greater than or equal to the geometric mean. Hence $\mathcal{W}(t) \leq 0$ and consequently, $D_{t_0}^\alpha \mathcal{W}(t) \leq 0$.

303 Moreover, the largest compact invariant set in $U_2 = \{(S^*, E^*, I^*, D^*, P^*) \in \Gamma : D_{t_0}^\alpha \mathcal{W}(t) = 0\}$

304 is a singleton set containing the endemic equilibrium \mathcal{E}^* , where $S(t) \equiv S^*$, $E(t) \equiv E^*$, $I(t) \equiv I^*$,

305 $D(t) \equiv D^*$, and $P(t) \equiv P^*$. Using Theorem (3.3), we conclude that the endemic equilibrium

306 point \mathcal{E}^* is globally asymptotically stable if $\mathcal{R}_0 > 1$. □

307 4 Numerical Simulations and Discussions

308 In this section, we performed the numerical simulations of the model (2) to justify the analytical
 309 results. Most of the parameter values which are not available in literature have been estimated
 310 within the reasonable realistic situation, the cumulative number of EVD monthly cases from
 311 March to August of the 2014 Ebola outbreak in Guinea was utilized (see [9]). We performed
 312 the numerical simulations using fractional Adam-Bashforth-Moulton scheme [47] as illustrated
 313 in equation (17):

314 For any differential equation:

$$315 \quad D_{t_0}^\alpha x(t) = g(t, x(t)), \quad 0 \leq t \leq T, \quad (17)$$

316 with the following initial conditions:

$$317 \quad x^i(0) = x_0^i, \quad i = 0, 1, 2, 3, \dots, [\alpha] - 1. \quad (18)$$

318 Operating by the fractional integral operator on equation (17) we obtain the solution $x(t)$ by
 319 solving equation (19):

$$320 \quad x(t) = \sum_{i=0}^{[\alpha]-1} \frac{x_0^i}{i!} t^i + \frac{1}{\Gamma(\alpha)} \int_0^t (t-\tau)^{\alpha-1} g(\tau, x(\tau)) d\tau. \quad (19)$$

321 Diethelm [58] used the predictor-corrector scheme based on the Adam-Bashforth-Moulton algo-
 322 rithm to numerically solve equation (19). Setting $h = \frac{T}{N}$, $t_n = nh$, and $n = 0, 1, 2, 3, \dots, N \in \mathbb{Z}^+$,
 323 we discretized equation (19) as a fractional variant of the one step Adam-Bashforth-Moulton
 324 scheme as shown in equation (20):

$$325 \quad x_h(t_{n+1}) = \sum_{i=0}^{[\alpha]-1} \frac{x_0^i}{i!} t_{n+1}^i + \frac{h^\alpha}{\Gamma(\alpha+2)} \sum_{q=0}^n a_{q,n+1} g(t_q, x_q) \\ + \frac{h^\alpha}{\Gamma(\alpha+2)} g(t_{n+1}, x_{n+1}^p), \quad (20)$$

$$326 \quad \text{where: } a_{q,n+1} = \begin{cases} n^{\alpha+1} - (n-\alpha)(n+\alpha)^\alpha, & q = 0, \\ (n-q+2)^{\alpha+1} + (n-q)^{\alpha+1} - 2(n-q+1)^{\alpha+1}, & 1 \leq q \leq n, \\ 1, & q = n+1, \end{cases}$$

327 and the predicted value $x_h^p(t_{n+1})$ is determined by:

$$328 \quad x_h(t_{n+1}) = \sum_{i=0}^{[\alpha]-1} \frac{x_0^i}{i!} t_{n+1}^i + \frac{1}{\Gamma(\alpha)} \sum_{q=0}^n b_{q,n+1} g(t_q, x_h(t_q)), \quad (21)$$

329 with:

$$330 \quad b_{q,n+1} = \frac{h^\alpha}{\alpha} ((n+1-q)^\alpha - (n-q)^\alpha). \quad (22)$$

331 The error estimate is:

$$332 \quad \max_{0 \leq q \leq k} |x(t_q) - x_h(t_q)| = O(h^p), \quad (23)$$

333 with $k \in \mathbb{N}$ and $p = \min(2, 1 + \alpha)$.

334 **4.1 Application of Adam-Bashforth-Moulton Scheme to the proposed mod-** 335 **el**

336 Most of the fractional order derivatives $\alpha \in (0, 1)$ that describe the real-world problems are
337 highly complicated and difficult to obtain its numerical approximations due to the existence of
338 their non-local in nature compared to the integer order derivatives. Adam-Bashforth-Moulton
339 scheme have been recognized as a powerful numerical scheme to solve nonlinear fractional order
340 problems due to its stability compared to other methods. Therefore, in this section we utilize
341 the Adam-Bashforth-Moulton scheme to numerically solve the nonlinear fractional model (2).
342 In the view to the generalized Adam-Bashforth-Moulton scheme, the proposed model (2) has
343 the following form:

$$\begin{aligned}
S(t_{n+1}) &= S_0 + \frac{h^\alpha}{\Gamma(\alpha+2)} (\Lambda^\alpha - (\beta_1^\alpha I^p(t_{n+1}) + \beta_2^\alpha D^p(t_{n+1}) + \lambda^\alpha P^p(t_{n+1})) S^p(t_{n+1}) \\
&\quad + \phi^\alpha E^p(t_{n+1}) - m_1 S^p(t_{n+1})) \\
&\quad + \frac{h^\alpha}{\Gamma(\alpha+2)} \sum_{q=0}^n a_{q,n+1} (\Lambda^\alpha - (\beta_1^\alpha I(t_q) + \beta_2^\alpha D(t_q) + \lambda^\alpha P(t_q)) S(t_q) \\
&\quad + \phi^\alpha E(t_q) - m_1 S(t_q)), \\
E(t_{n+1}) &= E_0 + \frac{h^\alpha}{\Gamma(\alpha+2)} (\psi^\alpha S^p(t_{n+1}) - \gamma^\alpha (\beta_1^\alpha I^p(t_{n+1}) + \beta_2^\alpha D^p(t_{n+1})) \\
&\quad + \lambda^\alpha P^p(t_{n+1})) E^p(t_{n+1}) - m_2 E^p(t_{n+1})) \\
&\quad + \frac{h^\alpha}{\Gamma(\alpha+2)} \sum_{q=0}^n a_{q,n+1} (\psi^\alpha S(t_q) - \gamma^\alpha (\beta_1^\alpha I(t_q) + \beta_2^\alpha D(t_q) \\
&\quad + \lambda^\alpha P(t_q)) E(t_q) - m_2 E(t_q)), \\
I(t_{n+1}) &= I_0 + \frac{h^\alpha}{\Gamma(\alpha+2)} ([(\beta_1^\alpha I^p(t_{n+1}) + \beta_2^\alpha D^p(t_{n+1}) + \lambda^\alpha P^p(t_{n+1})) S^p(t_{n+1}) \\
&\quad + \gamma^\alpha (\beta_1^\alpha I^p(t_{n+1}) + \beta_2^\alpha D^p(t_{n+1}) + \lambda^\alpha P^p(t_{n+1})) E^p(t_{n+1})] - m_3 I^p(t_{n+1})) \\
&\quad + \frac{h^\alpha}{\Gamma(\alpha+2)} \sum_{q=0}^n a_{q,n+1} ([(\beta_1^\alpha I(t_q) + \beta_2^\alpha D(t_q) + \lambda^\alpha P(t_q)) S(t_q) \\
&\quad + \gamma^\alpha (\beta_1^\alpha I(t_q) + \beta_2^\alpha D(t_q) + \lambda^\alpha P(t_q)) E(t_q)] - m_3 I(t_q)) \\
R(t_{n+1}) &= R_0 + \frac{h^\alpha}{\Gamma(\alpha+2)} (\sigma^\alpha I^p(t_{n+1}) - \mu^\alpha R^p(t_{n+1})) \\
&\quad + \frac{h^\alpha}{\Gamma(\alpha+2)} \sum_{q=0}^n a_{q,n+1} (\sigma^\alpha I(t_q) - \mu^\alpha R(t_q)) \\
D(t_{n+1}) &= D_0 + \frac{h^\alpha}{\Gamma(\alpha+2)} (m_4 I^p(t_{n+1}) - \epsilon^\alpha D^p(t_{n+1})) \\
&\quad + \frac{h^\alpha}{\Gamma(\alpha+2)} \sum_{q=0}^n a_{q,n+1} (m_4 I(t_q) - \epsilon^\alpha D(t_q)) \\
P(t_{n+1}) &= P_0 + \frac{h^\alpha}{\Gamma(\alpha+2)} (\rho^\alpha I^p(t_{n+1}) + \theta^\alpha D^p(t_{n+1}) - m_5 P^p(t_{n+1})) \\
&\quad + \frac{h^\alpha}{\Gamma(\alpha+2)} \sum_{q=0}^n a_{q,n+1} (\rho^\alpha I(t_q) + \theta^\alpha D(t_q) - m_5 P(t_q)),
\end{aligned} \tag{24}$$

346 where:

$$\left. \begin{aligned}
S^p(t_{n+1}) &= S_0 + \frac{h^\alpha}{\Gamma(\alpha)} \sum_{q=0}^n b_{q,n+1} (\Lambda^\alpha - (\beta_1^\alpha I(t_q) + \beta_2^\alpha D(t_q) + \lambda^\alpha P(t_q)) S(t_q) \\
&\quad + \phi^\alpha E(t_q) - m_1 S(t_q)), \\
E^p(t_{n+1}) &= E_0 + \frac{h^\alpha}{\Gamma(\alpha)} \sum_{q=0}^n b_{q,n+1} (\psi^\alpha S(t_q) - \gamma^\alpha (\beta_1^\alpha I(t_q) + \beta_2^\alpha D(t_q) \\
&\quad + \lambda^\alpha P(t_q)) E(t_q) - m_2 E(t_q)), \\
I^p(t_{n+1}) &= I_0 + \frac{h^\alpha}{\Gamma(\alpha)} \sum_{q=0}^n b_{q,n+1} ((\beta_1^\alpha I(t_q) + \beta_2^\alpha D(t_q) + \lambda^\alpha P(t_q)) S(t_q) \\
&\quad + \gamma^\alpha (\beta_1^\alpha I(t_q) + \beta_2^\alpha D(t_q) + \lambda^\alpha P(t_q)) E(t_q)) - m_3 I(t_q)), \\
R^p(t_{n+1}) &= R_0 + \frac{h^\alpha}{\Gamma(\alpha)} \sum_{q=0}^n b_{q,n+1} (\sigma^\alpha I(t_q) - \mu^\alpha R(t_q)) \\
D^p(t_{n+1}) &= D_0 + \frac{h^\alpha}{\Gamma(\alpha)} \sum_{q=0}^n b_{q,n+1} (m_4 I(t_q) - \epsilon^\alpha D(t_q)) \\
P^p(t_{n+1}) &= P_0 + \frac{h^\alpha}{\Gamma(\alpha)} \sum_{q=0}^n b_{q,n+1} (\rho^\alpha I(t_q) + \theta^\alpha D(t_q) - m_5 P(t_q)).
\end{aligned} \right\} \quad (25)$$

347

348 In simulating the model (2) we assume the initial condition that $S(0) = 10000$, $E(0) =$
349 290 , $I(0) = 10$, $R(0) = 50$, $D(0) = 0$ and $P(0) = 0$.

Table 2: Parameters and values

Symbol	Definition	Range/ Value	Units	Source
δ	Disease death rate	0.4-0.9	day^{-1}	[50, 59, 60]
η	Environmental decontamination rate	0.06	day^{-1}	fitted
β_1	Transmission rate of infectious humans	variable	day^{-1}	[59, 61, 62]
β_2	Transmission rate of deceased humans	variable	day^{-1}	[60, 62]
λ	Transmission rate of Ebola virus	variable	day^{-1}	fitted
τ	Pathogen decay rate	$(0, \infty)$	day^{-1}	[63, 64]
ρ	Shading rate of infectious humans	0.0004	day^{-1}	fitted
θ	Shading rate of deceased humans	0.004	day^{-1}	fitted
ϵ	Burial rate of deceased humans	$(0, 1)$	day^{-1}	[62, 65]
μ	Natural death rate	$(0, 1)$	day^{-1}	[66]
ϕ	Lost of education rate	0.025	day^{-1}	fitted
γ	Modification factor	0.7	-	fitted
Λ	Recruitment rate	variable	day^{-1}	fitted
ψ	Education rate	0.31	day^{-1}	fitted
σ	Recovery rate of humans	$(0, 1)$	day^{-1}	[59, 61, 62]

350 4.2 Sensitivity Analysis

351 In this section, we perform the sensitivity analysis of the model (2). The threshold quantity \mathcal{R}_0
352 known as basic reproduction number is an important parameter to determine the persistence
353 and extinction of EVD in the population. Parameter values of the Ebola model in Equation
354 (2) taken from literature as presented in Table 2 and while some are estimated, therefore,
355 sensitivity analysis will be useful on identifying parameters with greatest influence to change
356 the magnitude of threshold quantity \mathcal{R}_0 .

357 **Definition 2.** (See, [67]) *The normalized sensitivity index of \mathcal{R}_0 which depends on differen-*
358 *tiability of parameter ω is defined as equation (26):*

$$359 \Psi_{\omega}^{\mathcal{R}_0} = \frac{\partial \mathcal{R}_0}{\partial \omega} \times \frac{\omega}{\mathcal{R}_0}, \quad (26)$$

361 where ω is the generic parameter of system (2).

Table 3: Sensitivity index of the model (2)

Parameter	β_1	β_2	λ	ϕ
Index	+0.4154	+0.371	+0.2125	+0.0106
Parameter	σ	δ	ρ	θ
Index	-0.0107	-0.2939	+0.0023	+0.2102
Parameter	ψ	μ	γ	
Index	-0.0154	-0.1054	-0.1579	
Parameter	τ	η	ϵ	
Index	-0.008	0	-0.5823	

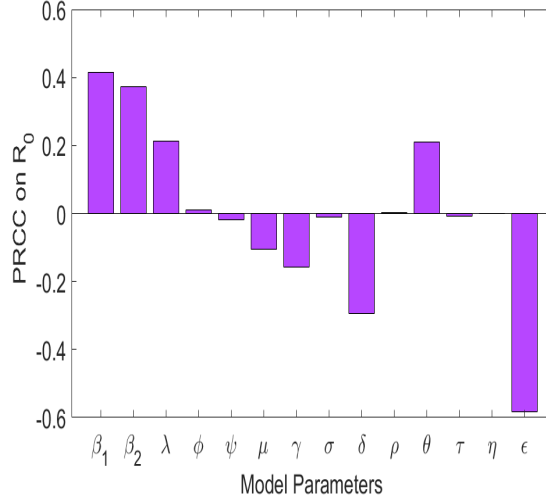


Figure 2: Sensitivity index of the model (2)

362 We observed that model parameters such as β_1 , β_2 , λ , ϕ , ρ , and θ , have a positive influence
363 on the magnitude of \mathcal{R}_0 , that is, whenever they are increased, the magnitude of \mathcal{R}_0 increases.
364 In Figure 2 it can be observed that an increase in the values of β_1 , β_2 , λ , ϕ , ρ , and θ by
365 10% increases the magnitude of \mathcal{R}_0 by 4.154%, 3.721%, 2.125%, 0.106%, 0.023%, and 2.102%,
366 respectively. While model parameters with negative index values have a negative influence on
367 the magnitude of \mathcal{R}_0 an increase in the values of ψ , μ , γ , σ , δ , τ and ϵ by 10% decreases the
368 magnitude of \mathcal{R}_0 by 0.154%, 1.054%, 1.579%, 0.107%, 2.939%, 0.08%, and 5.823%, respectively.
369 These results suggest that the burial rate of deceased humans ϵ , has the highest negative
370 influence on the magnitude of \mathcal{R}_0 . In addition, an increase in the indirect transmission rate of

371 Ebola virus λ , increases the magnitude of \mathcal{R}_0 .

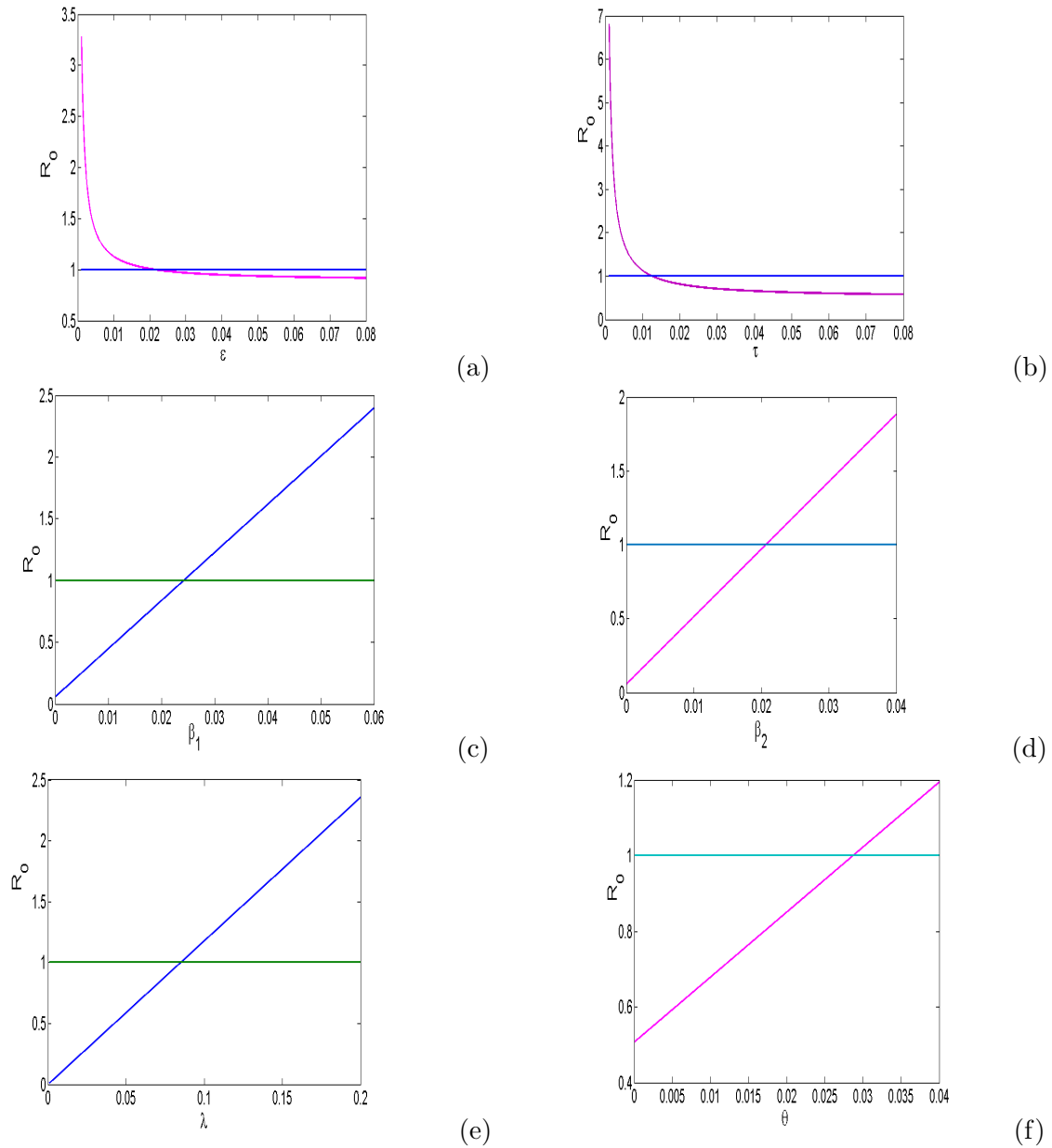


Figure 3: Numerical results of model (2) showing effects of varying (a) burial rate of deceased humans ϵ , on \mathcal{R}_0 (b) pathogen decay rate of Ebola virus τ , on \mathcal{R}_0 (c) transmission rate from infectious human β_1 , on \mathcal{R}_0 (d) transmission rate of deceased humans β_2 , on \mathcal{R}_0 (e) transmission rate of Ebola virus λ , on \mathcal{R}_0 (f) shading rate of deceased humans θ , on \mathcal{R}_0 .

372 We simulated model (2) to evaluate the effects of (a) burial rate of deceased humans ϵ , on
 373 \mathcal{R}_0 , at different values of ϵ , (b) pathogen decay rate of Ebola virus τ , on \mathcal{R}_0 , at different
 374 values of τ , (c) transmission rate from infectious human β_1 , on \mathcal{R}_0 , at different values of β_1

375 (d) transmission rate of deceased humans β_2 , on \mathcal{R}_0 , at different values of β_2 , (e) transmission
 376 rate of Ebola virus λ , on \mathcal{R}_0 , at different values of λ (f) shading rate of deceased humans θ ,
 377 on \mathcal{R}_0 , at different values of θ . The other parameters are fixed in all cases as in Table 3.
 378 The numerical results in Figure 3 (a) show burial rate of deceased humans ϵ , on \mathcal{R}_0 . We noted
 379 that increasing the burial rate on the deceased humans reduces the size of \mathcal{R}_0 . Additionally,
 380 whenever ϵ is greater than 0.02, the EVD dies in the community. In Figure 3 (b), we assess
 381 the effect of pathogen decay rate of Ebola virus τ , on \mathcal{R}_0 . We noted that whenever $\tau > 0.01$,
 382 the disease dies in the population. The numerical results in Figure 3 (c) show transmission
 383 rate from infectious β_1 , on \mathcal{R}_0 . We noted that increasing the transmission rate from infectious
 384 human increases the magnitude of \mathcal{R}_0 . In particular, whenever β_1 is greater than 0.025, the
 385 disease persists in the community. In Figure 3 (d), we investigated the influence of transmission
 386 rate of deceased humans β_2 , on \mathcal{R}_0 . We observed that whenever $\beta_2 > 0.02$, the disease persists
 387 in the population. The numerical results in Figure 3 (e) show transmission rate of Ebola virus
 388 λ , on \mathcal{R}_0 . We observed that increasing the transmission rate of Ebola virus increases the size
 389 of \mathcal{R}_0 . In particular, whenever λ is greater than 0.1, the disease persists in the community. In
 390 Figure 3 (f), we investigated the influence of shading rate of deceased humans θ , on \mathcal{R}_0 . We
 391 noted that whenever $\theta > 0.03$, the disease persists in the community.

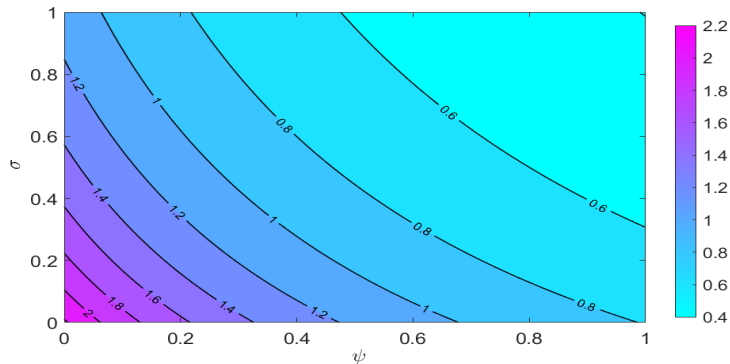


Figure 4: Numerical results of model (2) showing contour graph of \mathcal{R}_0 as the function of pre-
 vention measures and educational campaigns. We simulated the model (2) at $\epsilon = 0.074$, $\phi =$
 0.0004 , $\beta_1 = 1 \times 10^{-8}$, and $\beta_2 = 9.7 \times 10^{-6}$.

392 Figure 4 shows the contour graph of \mathcal{R}_0 as the function of educational campaigns and prevention
 393 measures. We simulated the model (2) at $\epsilon = 0.074$, $\phi = 0.0004$, $\beta_1 = 1 \times 10^{-8}$, and
 394 $\beta_2 = 9.7 \times 10^{-6}$. The results showed that as the rate of prevention measures and educational
 395 campaigns increases, the value of \mathcal{R}_0 decreases. This shows that both prevention measures

396 and educational campaigns have the potential to reduce the spread of EVD in the community.

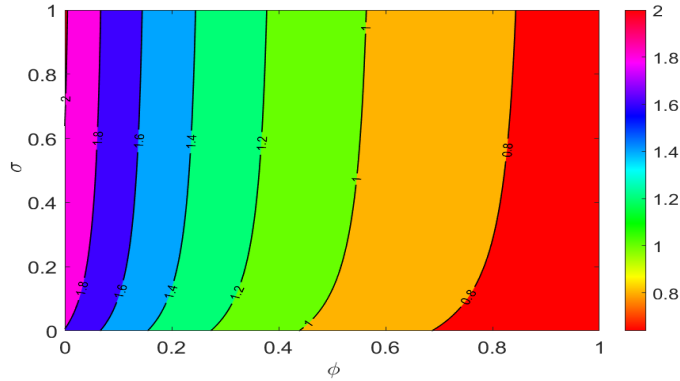


Figure 5: Numerical results of model (2) showing contour graph of \mathcal{R}_0 as the function of prevention measures and treatment of infected individuals. We simulated the model (2) at $\epsilon = 0.08$, $\psi = 0.025$, $\beta_1 = 1 \times 10^{-8}$, and $\beta_2 = 9.7 \times 10^{-6}$.

397 Figure 5 shows the contour graph of \mathcal{R}_0 as the function of prevention measures and recovery rate
 398 due to the treatment of infected individuals . We simulated the model (2) at $\epsilon = 0.08$, $\psi =$
 399 0.025 , $\beta_1 = 1 \times 10^{-8}$, and $\beta_2 = 9.7 \times 10^{-6}$. We observe that increasing the rate of prevention
 400 measures and recovery rate due to the treatment of infected individuals lead to decreased
 401 magnitude of \mathcal{R}_0 . This demonstrates the effect of prevention measures and treatment of
 402 infected individuals in reducing the transmission of Ebola in the population.

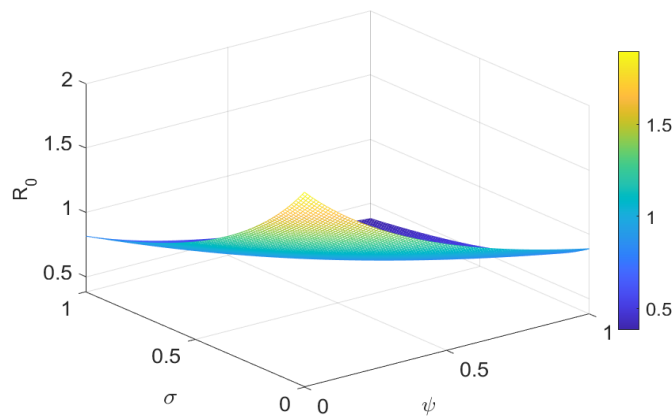


Figure 6: Mesh plot of \mathcal{R}_0 as the function of educational campaigns and recovery rate due to the treatment of infected individuals. We simulated the model (2) at $\epsilon = 0.094$, $\phi = 0.071$, $\beta_1 = 1 \times 10^{-8}$, and $\beta_2 = 9.7 \times 10^{-6}$.

403 Figure 6 shows the mesh plot of \mathcal{R}_0 as the function of educational campaigns and recovery rate
404 due to the treatment of infected individuals . We simulated the model (2) at $\epsilon = 0.094$, $\phi =$
405 0.071 , $\beta_1 = 1 \times 10^{-8}$, and $\beta_2 = 9.7 \times 10^{-6}$. It was noted that increasing the rate of educational
406 campaigns and recovery rate due to the treatment of infected individuals lead to decreased
407 magnitude of \mathcal{R}_0 . This demonstrates the effect of educational campaigns and treatment of
408 infected individuals reduce the transmission of Ebola in the population.

409 4.3 Parameter Estimation

410 In this section, we numerically solve the proposed model (2) and estimate the parameters η ,
411 λ , ρ , θ , ϕ , γ , Λ , ψ that minimize the deviation of real data from the prediction model (2) using
412 the least squares (RMSE) and Nelder mead algorithm techniques, and while the rest are fitted.
413 The real data of Ebola cases used are reported in [9]. Despite the challenges in model fitting
414 and parameter estimations, model fitting and parameter estimation in fractional order models
415 is an integral part in the disease modeling. The present data were reported in Guinea from
416 22 March to 16 August 2014, and the cumulative new infections predicted by the model (2) is
417 obtained using the equation (27):

$$418 \quad D_{t_0}^\alpha C(t) = (\beta_1^\alpha I(t) + \beta_2^\alpha D(t) + \lambda^\alpha P(t))(S(t) + \gamma^\alpha E(t)) \quad (27)$$

419 Further, we use the following function to compute the best fitting:

$$420 \quad \mathbb{F} : \mathbb{R}_{(\eta, \lambda, \rho, \theta, \phi, \gamma, \Lambda, \psi)}^8 \rightarrow \mathbb{R}_{(\eta, \lambda, \rho, \theta, \phi, \gamma, \Lambda, \psi)} \quad (28)$$

421 where $\eta, \lambda, \rho, \theta, \phi, \gamma, \Lambda, \psi$ are variables such that:

422 (1) For a given $(\eta, \lambda, \rho, \theta, \phi, \gamma, \Lambda, \psi)$, solve numerically the model differential equations (2) to
423 obtain a solution $\hat{Y}_i(t) = (\hat{S}, \hat{E}, \hat{I}, \hat{R}, \hat{P}, \hat{D})$ which is an approximation of the reported
424 Ebola cases $Y(t)$.

425 (2) Set $t_0 = 1$ (the model fitting starts in March 22) and for $t = 2, 3, \dots, 53$, corresponding to
426 the number of weeks where data are available, obtain the computed numerical solution
427 for $i_h(t)$; that is., $\hat{I}(1), \hat{I}(2), \hat{I}(3), \dots, \hat{I}(53)$.

428 (3) Compute the (RMSE) of the difference between $\hat{I}(1), \hat{I}_h(2), \dots, \hat{I}_h(53)$ and observed cases.

429 This function \mathbb{F} yields the RMSE where

$$430 \quad \text{RMSE} = \sqrt{\frac{1}{n} \sum_{k=1}^{53} (I(k) - \hat{I}(k))^2}, \quad (29)$$

431 (4) By using Nelder-Mead algorithm determine a global minimum for the RMSE .

432 The function \mathbb{F} takes values in \mathbb{R}^8 and yields a positive real number, the RMSE that measures
433 the closeness of the model predictions to the observed data. Using the formula in equation (29),
434 the *RMSE* was found to be 0.1353. This shows that the proposed model had 13.53% deviations
435 from observed values. It concluded that the model was approximately 86.47% efficient. On
436 performing the fitting process, we assume the following initial conditions $S(0) = 1000$, $E(0) =$
437 290 , $I(0) = 10$, $R(0) = 50$, $D(0) = 0$, and $P(0) = 0$ and the model parameters in Table (2).

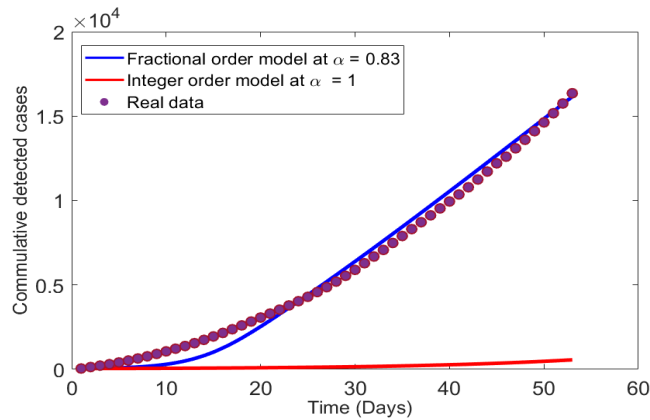
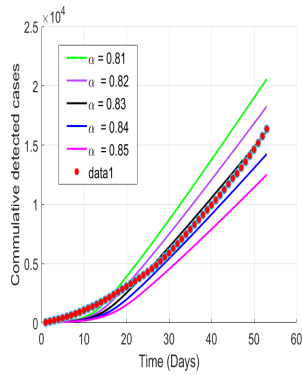
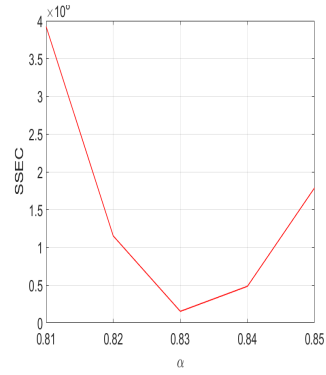


Figure 7: The model (2) fitted to Ebola cases reported in Guinea from 22 March to 16 August 2014 at $\alpha = 0.83$.

438 Figure 7 shows the cumulative detected cases of Ebola in Guinea. We used the monthly report
439 of Ebola cases reported in [9] to fit the model (2) at $\alpha = 0.83$. The results demonstrated
440 that the model (2) fits well the monthly Ebola cases reported in Guinea from 22 March to 16
441 August 2014 .



(a)



(b)

Figure 8: Numerical results of model 2 (a) shows the real data fitted at different order of derivatives (b) plots of order derivatives against the sum of square error cumulative (SSEC)

442 The numerical results in Figure 8 (a) shows the real data fitted with the fractional model at the
 443 order of derivatives $\alpha = 0.81, 0.82, 0.83, 0.84, 0.85$. We noted that the model had better fit at
 444 $\alpha = 0.83$. Figure (b), we plotted the variation of order of derivative against the sum of square
 445 error cumulative (SSEC). Overall, the model had minimum sum of square error cumulative at
 446 $\alpha = 0.83$ which agree with results in Figure (b). Thus, the model had better fits at $\alpha = 0.83$.

447 4.4 Numerical Results

448 Next, we simulate the model (2), we varied different model parameters and the order α of the
 449 caputo operator in order to explain the role of various parameters and memory index on the
 450 disease transmission patterns and control to support the analytical results. We first simulate
 451 the model at $\mathcal{R}_0 > 1$, followed by simulation at $\mathcal{R}_0 < 1$ to show the dynamics of the disease in
 452 the population.

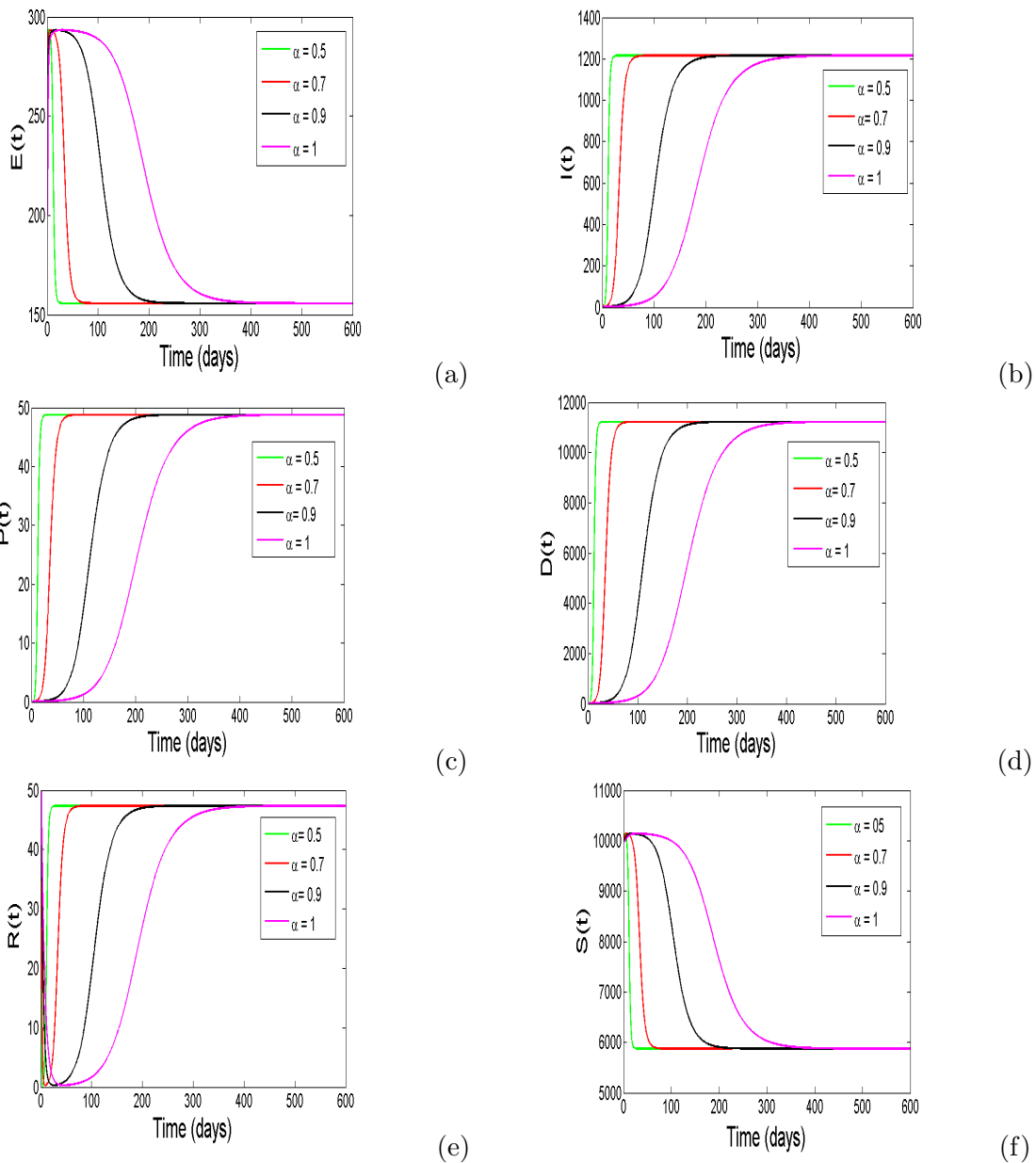


Figure 9: Simulation of the model (2) showing the convergence of infected individuals at the endemic equilibria point.

453 Figure 9 is a simulation of the model (2) to demonstrate the solution profile of individuals at
 454 the endemic equilibrium point. To explore the effects of different derivative orders, α , on the
 455 dynamics of the disease, we simulated the model at $\mathcal{R}_0 = 1.7520$, with the parameter values
 456 in Table 2 for $\alpha = 0.5$, $\alpha = 0.7$, $\alpha = 0.9$, and $\alpha = 1$. As we can note, with baseline
 457 values in Table 2, the disease will persist. Firstly, the results show that the variables for
 458 infected epidemiological compartments $I(t)$, $D(t)$, and $P(t)$ in Figure 9 (b), 9 (c), and 9 (d)

459 respectively, will increase the infection gradually and after about 300 days, the infection settle
 460 and attain stability at the endemic equilibrium at $I(t) \approx 1200$, $D(t) \approx 1050$, and $P(t) \approx 49$.
 461 A Similar pattern are observed for the compartment $R(t)$ in Figure (9)(e). In addition, the
 462 variables for susceptible epidemiological compartments $S(t)$, and $E(t)$ in Figure (9)(a), and
 463 (9)(f) respectively, show that susceptibility will decrease gradually and after about 300 days,
 464 the susceptibility settle and attain stability at the endemic equilibrium at $S(t) \approx 600$, and
 465 $E(t) \approx 290$. One can observe that as the value of the fractional-order α approaches unity,
 466 the time taken by model variables to converge to their respective unique endemic equilibrium
 467 point increases. These results agree with the analytical analysis of global stability for endemic
 468 equilibrium point in Theorem 3.4. It was further noted that at the fractional-order derivatives
 469 α , the human population attain its stability faster than at the classical integer.

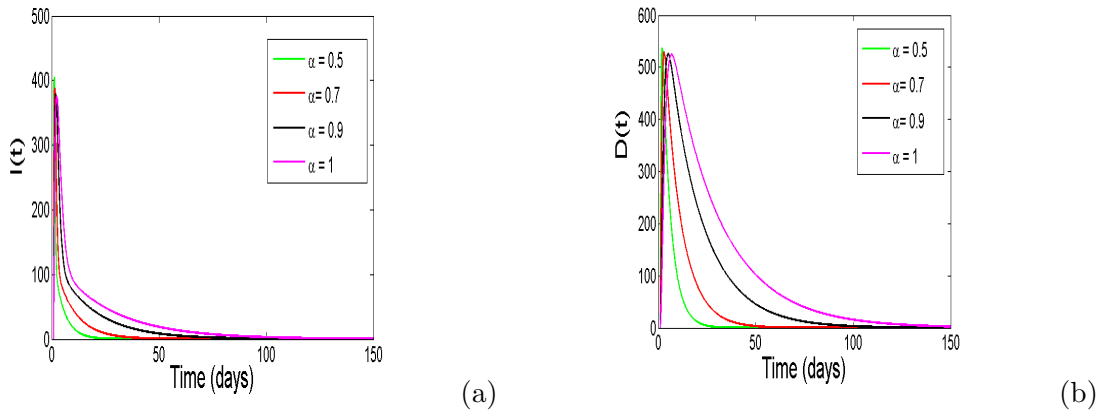


Figure 10: Simulation of the model (2) to show the convergence of infected humans and dead bodies at the disease free equilibrium point. We simulate the model (2) at $\mathcal{R}_0 = 0.6916$ with $\beta_1 = 1 \times 10^{-8}$, $\beta_2 = 9.7 \times 10^{-6}$, $\phi = 0.85$, $\psi = 0.71$. At different values of fractional-order derivatives, the number of infected individuals generated over the period of 150 days converge to the disease free equilibrium point.

470 Figure (10) shows the simulation of the model (2) to demonstrate the convergence of infected
 471 human population to the disease-free equilibrium point. To examine the effects of different
 472 derivative orders, α , on the dynamics of the disease, we simulated the model at $\mathcal{R}_0 = 0.6916$,
 473 with $\beta_1 = 1 \times 10^{-8}$, $\beta_2 = 9.7 \times 10^{-6}$, $\phi = 0.85$, $\psi = 0.71$ and the remainder retained the
 474 baseline values in Table 2 for $\alpha = 0.5$, $\alpha = 0.7$, $\alpha = 0.9$, and $\alpha = 1$. As we can note, with
 475 baseline values in Table 2, the disease will die. We can note that, the variables for infected epi-
 476 demiological compartments $I(t)$, and $D(t)$ in Figure 10 (a), and 10 (b), respectively, show that
 477 the infection will decrease gradually and after about 100 days, the infection settle and attain

478 stability at the disease-free equilibrium at $I(t) = 0$, and $D(t) = 0$. Furthermore, as the value of
 479 the fractional-order α approaches unity, the time taken by the model variables to converge to
 480 their respective unique disease-free equilibrium point increases. The results demonstrate that
 481 in a long-range interaction of people in the population, all infected individuals converge to one
 482 point which is the disease-free equilibrium point. This agrees with the analytical results on
 483 the existence of global stability for disease-free equilibrium point for the model (2) in Theorem
 484 3.5. Also we have noted that as the fractional-order derivatives α decrease from integer and
 485 infected humans attain stability much faster than at $\alpha = 1$. This shows the importance of
 486 using fractional-order derivatives in modeling biological systems.

487 5 Concluding Remarks

488 In this article, a Caputo derivative model for EVD with intervention strategies is proposed
 489 and analyzed. A Majority of mathematical models for EVD in literature are based on integer-
 490 ordinary differential equations, and much has not been done to investigate the role of memory
 491 effects on EVD dynamics. Thus, the main aim of this study was to develop a more realistic
 492 EVD model that incorporate memory effects. The formulated model subdivides the total
 493 human population based on epidemiological status as susceptible population unaware of the
 494 disease fighting, susceptible population aware of disease fighting; infected individuals who are
 495 clinically displaying signs of the disease and are infectious, individuals who have recovered
 496 from infection, and deceased population. The studied model has an additional compartment
 497 that captures the concentration of pathogens in the environment. We perform the sensitivity
 498 analysis to demonstrate the influence of each parameter on the magnitude of threshold quantity
 499 \mathcal{R}_0 . The results show that that model parameters such as β_1 , β_2 , λ , ϕ , ρ , and θ , have a positive
 500 correlation with the magnitude of \mathcal{R}_0 , that is, whenever they are increased, the magnitude
 501 of \mathcal{R}_0 increases. Furthermore, an increase in the values of β_1 , β_2 , λ , ϕ , ρ , and θ by 10%
 502 will increase the magnitude of \mathcal{R}_0 by 4.154%, 3.721%, 2.125%, 0.106%, 0.023%, and 2.102%,
 503 respectively. While model parameters with negative index values have a negative correlation
 504 with the magnitude of \mathcal{R}_0 , we observed that an increase in the values of ψ , μ , γ , σ , δ , τ and
 505 ϵ by 10% decreases the magnitude of \mathcal{R}_0 by 0.154%, 1.054%, 1.579%, 0.107%, 2.939%, 0.08%,
 506 and 5.823%, respectively. These results suggest that the burial rate of deceased humans ϵ , has
 507 the highest negative influence on the magnitude of \mathcal{R}_0 . In addition, an increase in the indirect
 508 transmission rate of Ebola virus λ , will increase the magnitude of \mathcal{R}_0 .

509 The analytical results obtained in this study demonstrate that the fractional-order model
510 has a globally asymptotically stable disease-free equilibrium whenever $\mathcal{R}_0 < 1$. However, if
511 $\mathcal{R}_0 > 1$, the fractional-order model has an endemic equilibrium which is globally asymptotically
512 stable.

513 Subsequently, we fitted the model parameters with the Ebola cases reported in Guinea from
514 22 March to 16 August 2014 at $\alpha = 0.82, 0.83, 0.84$ and 0.85 . From our numerical results,
515 the model fits well with cases reported and health education campaigns, prevention measures
516 and treatments have the potential to minimize the spread of Ebola in the population. As the
517 memory effect α decreases from unity, the solution profiles of the model (2) attain stability
518 much faster than at $\alpha = 1$. In addition, the different values of the fractional-order have no effect
519 on the stability of the model (2) but influence the time taken for stability to be attained. These
520 results demonstrate the importance of fractional-order over the classical integer in modeling
521 biological systems.

522 As the modelling of EVD is not sufficiently developed, this work offers many opportunities
523 in improvements for future research where the model can be extended to incorporate a patch
524 structure to account for the circulation of the disease in many countries as it is the case in
525 Western Africa. In addition we expect to improve this study in the future by developing EVD
526 model(s) with a time delay that will enable the comparison of the Caputo derivative and time
527 delay approach

528

529 **Acknowledgment**

530 All authors are grateful to their respective institutions for the support during preparation of
531 the manuscript. Dr. Paride O. Lolika thank professor Yosa Wawa for his invaluable discussions
532 and comments during the preparation of this manuscript.

533 **Conflict of interest**

534 The authors declare that they have no conflicts of interest

535 **Authors Contributions**

536 All authors have equal contributions and they read and approved the final version of the paper.

537 References

- 538 [1] P. Rouguet, J.-M. Bermejo, A. Kilbourne, W. Karesh, P. Reed, B. Kumulunui, P. Yaba,
539 A. Delicat, P.E. Rollin, E.M. "Leroy, Wild animal mortality monitoring and human Ebola
540 outbreak, Gabon and republic of Congo, 2001-2003", *Emerg, infect. Dis*, 11,283-290,
541 2005.
- 542 [2] T. Smith, "Ebola and Marbug Virus (Deadly Disease and epidemics), second ed.",
543 *Chelsea House Pub*, 2010.
- 544 [3] WHO, "Ebola data and statistics," [http://apps.who.int/gho/data/view ebola-sitrep ebola-](http://apps.who.int/gho/data/view ebola-sitrep ebola-summary-20160511?lang=en)
545 [summary-20160511?lang=en.](http://apps.who.int/gho/data/view ebola-summary-20160511?lang=en), 2016.
- 546 [4] M.F. Jalloh, W. Li, R.F. Bunnell, et al, "Impact of Ebola experiences and risk perceptions
547 on mental health in Sierra Leone, July 2015", *BMJ Global Health*, 3:e000471, 2018.
- 548 [5] P. Richards, J. Amara, M.C. Ferme, P. Kamar, E. Mokuwa, A.I. Sheriff, R. Suluku , M.
549 Voors Marten, "Social pathways for Ebola virus disease in rural Sierra Leone and some
550 implications for containment", *PLOS Negl Trop Dis.*, 8(7):e3056, 2014.
- 551 [6] A. Manguvo, and B. Mafuvadze, "The impact of traditional and religious practices on
552 the spread of Ebola in West Africa: time for a strategic shift", *The Pan African medical*
553 *journal*, 22 Suppl 1(Suppl 1), 9. doi:10.11694/pamj.suppl.2015.22.1.6190, 2015.
- 554 [7] S. Hewlett Barry, P. Amola Richard, "Cultural contexts of Ebola in northern Uganda",
555 *Emerg Infect Dis.*; 9(10):1242, 2003.
- 556 [8] World Health Organization, "Global alert and response", 2014.
- 557 [9] C.L. Althaus, "Estimating the reproduction number of Ebola virus (EBOV) during the
558 2014 outbreak in West Africa", *PLoS Currents Outbreaks*, 6 (2014), 2014.
- 559 [10] M.V. Barbarossa, A. Denes, G. Kiss, Y. Nakata, G. Rost, & Z. Vizi, "Transmission
560 dynamics and final epidemic size of Ebola Virus Disease outbreaks with varying inter-
561 ventions", *PLoS One* ,10(7), e0131398, 2015.
- 562 [11] T. Berge, J.M.-S. Lubuma, G. M. Moremedi, N. Morris and R. Kondera-Shava, "A
563 simple mathematical model of Ebola in Africa", *Journal of Biological Dynamics*, 11:1,
564 42-74,DOI: 10.1080/17513758.20161229817, 2017.

- 565 [12] N. T. J. Bailey, and others. The mathematical theory of infectious diseases and its
566 applications, Charles Griffin & Company Ltd, 5a Crendon Street, High Wycombe, Bucks
567 HP13 6LE., 1975.
- 568 [13] R. M. Anderson. The population dynamics of infectious diseases: theory and applications,
569 Springer, 2013.
- 570 [14] H. R. Thieme. Convergence results and a Poincare-Bendison trichotomy for asymptotical
571 autonomous differential equations. *J. Math. Biol.* 30, 755-763, 1992.
- 572 [15] W. Wang and X-Q Zhao. Threshold dynamics for compartment epidemic models in
573 periodic environments. *Journal of Dynamics and Differential Equations*, 20:699-717, 2008.
- 574 [16] S. F. Dowel. Seasonal Variation in Host Susceptibility and Cycles of Certain Infectious
575 Diseases. *Emerging Infectious Diseases* 7: 369-374, 2001.
- 576 [17] Shuai, Z, Heesterbeek, J.A.P., van den Driessche, P. Extending the type reproduction
577 number to infectious disease control targeting contacts between types, *J. Math. Biol.* 67
578 (5)1067-1082, 2013.
- 579 [18] P. Van den Driessche and J. Watmough. Reproduction number and subthresh-
580 old endemic equilibria for compartment models of disease transmission. *Mathematical*
581 *Biosciences*, 180:29-48, 2002.
- 582 [19] Erinle-Ibrahim Latifat M. , Idowu K. Oluwatobi , and Sulola Abigail I (2021) Mathemat-
583 ical modelling of the transmission dynamics of malaria infection with optimal control.
584 *Kathmandu University Journal of Science, Engineering and Technology*, Vol. 15, No. 3,
585 December 2021.
- 586 [20] Idowu Kabir Oluwatobi1, Loyinmi Adedapo Chris (2023) Impact of Contaminated Sur-
587 faces on the Transmission Dynamics of Corona Virus Disease (Covid-19). *Journal of*
588 *Science Technical Research*, DOI: 10.26717/BJSTR.2023.51.008046
- 589 [21] Idowu Kabir Oluwatobi, Erinle-Ibrahim L.M (2021) Mathematical modelling of p-
590 neumonia dynamics of children under the age of five. *Research Square*, DOI:
591 <https://doi.org/10.21203/rs.3.rs-194578/v1>.

- 592 [22] Idowu Kabir Oluwatobi, Loyinmi Adedapo Chris (2023) Qualitative Analysis of the
593 Transmission Dynamics. Research Square, and Optimal Control of Covid-19, DOI:
594 <https://doi.org/10.21203/rs.3.rs-2707554/v1>
- 595 [23] M. Saeedian, and M. Khalighi, and N. Azimi-Tafreshi and G.R. Jafari, and M. Aus-
596 loos. Memory effects on epidemic evolution: The susceptible-infected-recovered epidemic
597 model, Physical Review E, Vol. 95, no. 2, pp. 022409, 2017.
- 598 [24] N. Hamdan, and A. Kilicman. Analysis of the fractional order dengue transmission model:
599 a case study in Malaysia, Springer, Vol. no.1, pp. 1-13, 2019.
- 600 [25] A. Mouaouine, and A. Boukhouima, and K. Hattaf, and N. Yousfi. A fractional order
601 SIR epidemic model with nonlinear incidence rate, Springer, pp. 1-9, 2018.
- 602 [26] J-G. Liu, X-J. Yang, Y-Y. Feng, L-L. Geng. Fundamental results to the weighted Caputo-
603 type differential operator. Applied Mathematics Letters 121, 107421, 2021.
- 604 [27] F.A. Rihan, and Q.M. Al-Mdallal, and H.J. AlSakaji, and A. Hashish. A fractional-order
605 epidemic model with time-delay and nonlinear incidence rate, Elsevier, Vol. 126, pp.
606 97-105, 2019.
- 607 [28] Vargas-De-Leó n., Volterra-type Lyapunov functions for fractional-order epidemic sys-
608 tems. Commun, *Nonlinear Sci. Numer. Simul.* **24**, 7585, 2015.
- 609 [29] M. Helikumi, M. Kgosimore, D. Kuznetsov, and S. Mushayabasa. A fractional-order Try-
610 panosoma brucei rhodesiense model with vector saturation and temperature dependent
611 parameters, Springer, no. 1, pp. 1-23, 2020.
- 612 [30] I. Area, H. Batarfi, J. Losada, J. J. Nieto, W. Shammakh , & A. Torres . "On a fractional
613 order Ebola epidemic model", *Advances in Difference Equations*, 2015(1), 1-12, 2015.
- 614 [31] M. Farman, A. Akgül, T. Abdeljawad, and P. A. Naik, and N. Bukhari, and A. Ahmad.
615 Modeling and analysis of fractional order Ebola virus model with Mittag-Leffler kernel,
616 Elsevier, Vol.61, no.3,pp. 2061-2073, 2022.
- 617 [32] M. A. Dokuyucu, and H. Dutta. A fractional order model for Ebola Virus with the new
618 Caputo fractional derivative without singular kernel, Elsevier, Vol. 134, pp. 109717, 2020.

- 619 [33] A. Raza, M. Farman, A. Akgül, M. S. Iqbal, and A. Ahmad. Simulation and numerical so-
620 lution of fractional order Ebola virus model with novel technique, AIMS Bioengineering,
621 Vol. 7, no. 4, pp. 194-207, 2020.
- 622 [34] H. Singh, "Analysis for fractional dynamics of Ebola virus model", *Chaos, Solitons &*
623 *Fractals*, 138, 109992, 2020.
- 624 [35] W. Pan, T. Li, and S. Ali. A fractional order epidemic model for the simulation of
625 outbreaks of Ebola, Springer, pp. 1-21, 2021.
- 626 [36] H. L. Li, L. Zhang, C. Hu, Y. L. Jiang, Z. Teng. Dynamical analysis of a fractional-order
627 predator-prey model incorporating a prey refuge. *Journal of Applied Mathematics and*
628 *Computing*, 54(1-2), 435-449, 2017.
- 629 [37] L.C. de Barros, M.M. Lopes, F. Santo Pedro, E. Esmi, J.P.C. dos Santos, and D.E.
630 Snchez. The memory effect on fractional calculus: an application in the spread of COVID-
631 19. *Computational and Applied Mathematics*, 40(3), pp.1-21, 2021.
- 632 [38] J. Huo, H. Zhao, L. Zhu . The effect of vaccines on backward bifurcation in a fractional
633 order HIV model. *Nonlinear Analysis: Real World Applications*, 26, 289-305, 2015.
- 634 [39] P. A. Naik, J. Zu, K. M. Owolabi. Global dynamics of a fractional order model for the
635 transmission of HIV epidemic with optimal control. *Chaos, Solitons & Fractals*, 138,
636 109826, 2020.
- 637 [40] K. M. Owolabi. Behavioural study of symbiosis dynamics via the Caputo and Atangan-
638 aBaleanu fractional derivatives. *Chaos, Solitons & Fractals*, 122, 89-101, 2019.
- 639 [41] K. M. Owolabi, A. Atangana. Mathematical analysis and computational experiments for
640 an epidemic system with nonlocal and nonsingular derivative. *Chaos, Solitons & Fractals*,
641 126, 41-49, 2019.
- 642 [42] Z. U. A. Zafar, K. Rehan, M. Mushtaq. HIV/AIDS epidemic fractional-order model.
643 *Journal of Difference Equations and applications*, 23(7), 1298-1315, 2017.
- 644 [43] K. Muhammad Altaf, & A. Atangana, "Dynamics of Ebola disease in the framework of
645 different fractional derivatives", *Entropy*, 21(3), 303, 2019.
- 646 [44] Z. Juan and M. Zhien. Global dynamics of an seir epidemic model with saturating contact
647 rate, *Mathematical Biosciences Journal*; 185,15-32, 2003.

- 648 [45] F. Nielsen Carie, S. Kidd, A.R. Sillah, E. Davis, J. Mermin, H. Kilmarx Peter, "Improving
649 burial practices and cemetery management during an Ebola virus disease epidemic-Sierra
650 Leone, 2014", *MMWR.*, 64(1):20, 2015.
- 651 [46] H.W. Berhe, S. Qureshi, and A. A. Shaikh. "Deterministic modeling of dysentery diar-
652 rhea epidemic under fractional Caputo differential operator via real statistical analysis",
653 *Chaos, Solitons & Fractals*, 131, p.109536, 2020.
- 654 [47] B. S. Alkahtani. Atangana-Batogna numerical scheme applied on a linear and non-linear
655 fractional differential equation, *The European Physical Journal Plus*, vol. 133, no. 3, pp.
656 110, 2018.
- 657 [48] J. Huo, H. Zhao, and L. Zhu. The effect of vaccines on backward bifurcation in a fractional
658 order HIV model, *Nonlinear Analysis: Real World Applications*, vol. 26, pp. 289305, 2015.
- 659 [49] H. Delavari, D. Baleanu, J. Sadati. "Stability analysis of Caputo fractional-order", *Non-*
660 *linear systems revisited, Nonlinear Dyn.*, **67**, 2433-2439, 2012.
- 661 [50] F.B. Aguston, M.I. Teboh-Wwaungkem, and A.B. Gumel, "Mathematical assessment of
662 the effect of traditional beliefs and customs on the transmission dynamics of the 2014
663 Ebola outbreak", *BMC MED.*, 13, p.96, 2015.
- 664 [51] B. Ivorra, D. Ngom and A.M. Ramos, Be-CodiS, "A mathematical model to predict
665 the risk of human diseases spread between countries-validation and application to the
666 2014-2015 ebola virus disease epidemic", *Bull. Math. Bio.* 77, pp 1668-1704, 2015.
- 667 [52] Li C, Zeng F (2013) The finite difference methods for fractional ordi-
668 nary differential equations. *Numer Funct Anal Optim* 34: 149-179. [http-](http://doi.org/10.1080/01630563.2012.706673)
669 [s://doi.org/10.1080/01630563.2012.706673](http://doi.org/10.1080/01630563.2012.706673)
- 670 [53] Liang S, Wu R, Chen L (2015) Laplace transform of fractional order differential equations.
671 *Electron J Differ Equ* 139: 2015. <http://ejde.math.txstate.edu>
- 672 [54] Kexue L, Jigen P (2011) Laplace transform and fractional differential equations. *Appl*
673 *Math Lett* 24: 2019-2023. <https://doi.org/10.1016/j.aml.2011.05.035>
- 674 [55] Podlubny I (1999) Fractional Differential Equations: An Introduction to Fractional
675 Derivatives, Fractional Differential Equations, to Methods of their Solution and some of

- 676 their Applications *Math Sci Eng* 7: 1-340. [https://doi.org/10.1016/s0076-5392\(99\)x8001-](https://doi.org/10.1016/s0076-5392(99)x8001-)
677 5
- 678 [56] Chen M and Wu R, Dynamics of a depletion-type Gierer-Meinhardt model with
679 Langmuir- Hinshelwood reaction scheme. *Discrete and Continuous Dynamical Systems*
680 *Series B* 27(4) (2022) 22752312.
- 681 [57] Khalil, H. K., *Nonlinear Systems* (Third edition), Prentice Hall, Englewood Cliffs, NJ,
682 2002.
- 683 [58] K. Diethelm, *The Analysis of Fractional Differential Equations: An Application-Oriented*
684 *Exposition Using Differential Operators of Caputo Type*, Springer Science & Business
685 Media, 2020.
- 686 [59] G. Chowell, N.W. Hengartner, C. Castillo-Chavez, P. W. Fenimore, and J.M. Hyman,
687 "The basic reproductive number of Ebola and the effects of public health measures: The
688 cases of Congo and Uganda", *J. Theo. Biol.*, 229, pp. 119-126, 2014.
- 689 [60] D. Fisman, E. Khoo, and A. Tuite, "Early epidemic dynamics of the the West
690 African 2014 Ebola outbreak: Estimates derived with a simple two Parameter mod-
691 el", *PLOS Curr. outbreaks*, sep 8. Edition 1 doi; 10.1371/ currents. outbreaks.
692 89cod3783f36958d96ebbae97348d571, 2014.
- 693 [61] J. Legrand, R.F. Grais, P.Y. Boelle, A.J. Valleron, and A. Flahault, "Understanding thd
694 dynamics of Ebola epidemics", *Epidemiol. Infect.*, 135, pp. 610-621, 2007.
- 695 [62] S. Towers, O. Patterson-Lomba, and C. Castillo-Chavez, "Temporal variations in the
696 reproduction number of the 2014 outbreaks", *PLOS Curr. outbreaks*, September 18,
697 2014.
- 698 [63] K. Bibby, L.W. Casson, E. Stachler, and C.N. Haas, "Ebola virus persistence in the
699 environment state of the knowledge and research needs", *Environ. Sci. Technol. Lett.*
700 *2.*, pp. 2-6, 2015.
- 701 [64] T.J. Piercy, S. J. Smither, J. A. Steward, L. Eastaugh, and M.S. Lever, "The Survival
702 of filoviruses in liquids, on solid substrate and in a dynamic aerosol", *J. App. Microbio.*,
703 109(5), pp. 1531-1539, 2010.

- 704 [65] F.O Fasina, A. Shitu, D. Lazarus, O. Tomori, L. Simonsen, C. Viboud, and G.
705 Chowell, "Transmission dynamics and control of Ebola virus disease outbreak in
706 Nigeria, July to September 2014", *Euro Surveill.*, 19 (40): pii 20920. Available at:
707 <http://www.eurosurveillance.org/ViewArticle.aspx?ArticleId=20920>, 2014.
- 708 [66] D. Ndanguza, J.M. Tchuenche, and H. Haario, "Statistical data analysis of the 1995
709 outbreak in the Democratic Republic of Congo", *Afrika Mat.*, 24, pp. 55-68, 2013.
- 710 [67] L. Arriola, and Hyman, J., "Forward and adjoint sensitivity analysis with applications
711 in dynamical systems", *Lecture Notes in Linear Algebra and Optimization*, 2005.

712 **Appendix A: Mathematical concepts of fractional order**

713 Consider the following differential equation of any dynamical system:

$$714 \quad \frac{df(t)}{dt} = \beta f(t) \quad (30)$$

715 where β is any constant or parameter. In order to capture the influence of memory effects, we
716 rewrite the differential equation (30) in terms of dependent integral as follows:

$$717 \quad \frac{df(t)}{dt} = \beta \int_{t_0}^t k(t - \xi) f(\xi) d\xi \quad (31)$$

718 In this case, $k(t - \xi)$ plays the role of the time dependent kernel and is equivalent to a delta
719 $\delta(t - \xi)$ in a classical Markov process. This type of kernel provides the existence of important
720 features which exist in real problems. Now let us consider the following power-law correlation
721 function for $k(t - \xi)$:

$$722 \quad k(t - \xi) = \frac{1}{\Gamma(\alpha - 1)} (t - \xi)^{\alpha - 2} \quad (32)$$

723 where $\Gamma(\alpha)$ denotes the Gamma function and $0 < \alpha \leq 1$. In this case, the choice of coefficient
724 $\Gamma(\alpha - 2)$ and the exponent $\alpha - 1$ allow to write the differential equation (30) to the form of
725 fractional order derivative in Caputo sense. Substituting this kernel in (30) the right hand side
726 of function leads to the fractional integral of order $(\alpha - 1)$ on the interval $[b, t]$, denoted by
727 ${}_b D_{t_0}^{-(\alpha - 1)}$. Applying a fractional Caputo derivative of order $(\alpha - 1)$ in (30) and using the fact
728 that both Caputo fractional derivative and fractional integral are inverse operators, one gets
729 the following fractional differential equation:

$$730 \quad D_{t_0}^\alpha f(t) = \beta^\alpha f(t) dt \quad (33)$$

731 where $D_{t_0}^\alpha f(t)$ denotes the Caputo fractional derivative of order $\alpha \in (0, 1)$, defined for an
 732 arbitrary function $f(t)$ as:

$$733 \quad D_{t_0}^\alpha f(t) = \frac{1}{\Gamma(1-\alpha)} \int_0^t \frac{\dot{f}(\xi)}{(t-\xi)^\alpha} d\xi. \quad (34)$$

734 Thus, the function (34) defines the fractional order derivatives in Caputo sense.

735 *Remarks* : Note that, In order to avoid flaws regarding the time dimension, we introduce the α
 736 in parameter β (right-hand side) of the differential equation (33) so that the dimension of the
 737 parameter β become $(time)^{-\alpha}$ which agree with the left-hand side of the differential equation.

738 **Definition 3.** For the differential equation described in (30)

739 (i) The trivial solution is said to be stable if, for every $t_0 \in \mathbb{R}$ and every $\epsilon > 0$, there exists
 740 $\delta = \delta(t_0, \epsilon)$ such that $\|x(t_0)\| < \delta \rightarrow \|x(t)\| < \epsilon$ for all $t > t_0$.

741 (ii) The trivial solution is said to be asymptotically stable if it is stable and, for any $t_0 \in \mathbb{R}$
 742 and any $\epsilon > 0$, there exists $\delta_a = \delta_a(t_0, \epsilon) > 0$ such that $\|x(t)\| < \delta_a \rightarrow \lim_{t \rightarrow \infty} \|x(t)\| = 0$

743 (iii) The trivial solution is said to be uniformly stable if it is stable and $\delta = \delta(\epsilon) > 0$ can be
 744 chosen independently of t_0 .

745 (iv) The trivial solution is uniformly asymptotically stable if it is uniformly stable and there
 746 exists δ_a independently of t_0 , such that if $\|x(t)\| < \delta_a$, then $\lim_{t \rightarrow \infty} \|x(t)\| = 0$.

747 (iii) The trivial solution is said to be uniformly stable if it is stable and $\delta = \delta(\epsilon) > 0$ can be
 748 chosen independently of t_0 .

749 (v) The trivial solution is globally asymptotically stable if it is asymptotically stable and
 750 δ_a can be any arbitrarily large finite number.

751 Appendix B: Non-negativity and boundedness of model solutions

752 In this section, we present the existence, uniqueness, positivity and boundedness of the solu-
 753 tions of model (2). We commence our discussion by demonstrating existence and uniqueness
 754 of solutions. Our approach is based on the fixed-point theory. Let \mathcal{B} be a Banach space of
 755 real-valued continuous functions defined on an interval \mathcal{I} with the associated norm:

$$756 \quad \|S, E, I, R, D, P\| = \|S\| + \|E\| + \|I\| + \|R\| + \|D\| + \|P\| \quad (35)$$

757 where $\|S\| = \sup\{|S(t)| : t \in \mathcal{I}\}$, $\|E\| = \sup\{|E(t)| : t \in \mathcal{I}\}$, $\|I\| = \sup\{|I(t)| : t \in \mathcal{I}\}$,
 758 $\|R\| = \sup\{|R(t)| : t \in \mathcal{I}\}$, $\|D\| = \sup\{|D(t)| : t \in \mathcal{I}\}$, $\|P\| = \sup\{|P(t)| : t \in \mathcal{I}\}$, and

759 $\mathcal{B} = \mathcal{E}(\mathcal{I}) \times \mathcal{E}(\mathcal{I}) \times \mathcal{E}(\mathcal{I}) \times \mathcal{E}(\mathcal{I}) \times \mathcal{E}(\mathcal{I}) \times \mathcal{E}(\mathcal{I}) \times \mathcal{E}(\mathcal{I})$, with $\mathcal{E}(\mathcal{I})$ denoting the Banach space
760 of real-valued continuous functions on \mathcal{I} and the associated sup norm. The model system (2)
761 can be rewritten in the the following form:

$$\left. \begin{aligned}
 D_{t_0}^\alpha S(t) &= G_1(t, S), \\
 D_{t_0}^\alpha E(t) &= G_2(t, E), \\
 D_{t_0}^\alpha I(t) &= G_3(t, I), \\
 D_{t_0}^\alpha R(t) &= G_4(t, R), \\
 D_{t_0}^\alpha D(t) &= G_5(t, D), \\
 D_{t_0}^\alpha P(t) &= G_6(t, P),
 \end{aligned} \right\}. \quad (36)$$

763 By applying the Caputo fractional integral operator, system (36), reduces to the following
764 integral equation of Volterra type with Caputo fractional integral of order $0 < \alpha < 1$,

$$\left. \begin{aligned}
 S(t) - S(0) &= \frac{1}{\Gamma(\alpha)} \int_0^t (t - \chi)^{\alpha-1} G_1(\chi, S) d\chi, \\
 E(t) - E(0) &= \frac{1}{\Gamma(\alpha)} \int_0^t (t - \chi)^{\alpha-1} G_2(\chi, E) d\chi, \\
 I(t) - I(0) &= \frac{1}{\Gamma(\alpha)} \int_0^t (t - \chi)^{\alpha-1} G_3(\chi, I) d\chi, \\
 R(t) - R(0) &= \frac{1}{\Gamma(\alpha)} \int_0^t (t - \chi)^{\alpha-1} G_4(\chi, I) d\chi, \\
 D(t) - D(0) &= \frac{1}{\Gamma(\alpha)} \int_0^t (t - \chi)^{\alpha-1} G_5(\chi, D) d\chi, \\
 P(t) - P(0) &= \frac{1}{\Gamma(\alpha)} \int_0^t (t - \chi)^{\alpha-1} G_6(\chi, P) d\chi,
 \end{aligned} \right\} \quad (37)$$

766 What follows, we prove that the kernels G_i , $i = 1, 2, 3, 4, 5, 6$ fulfill the Lipschitz condition and
767 contraction under some assumptions. In the following theorem, we have demonstrated for G_1
768 and one can easily verify for the remainder.

769 **Theorem 5.1.** *Let us consider the following inequality*

$$0 \leq (\beta_1 k_1 + \beta_2 k_2 + \lambda k_3 + \mu + \psi) < 1.$$

771 *The kernel G_1 satisfies the Lipschitz condition as well as contraction if the above inequality is*
772 *satisfied.*

773 *Proof.* For S and S_1 we proceed as below.

$$\begin{aligned}
 \|G_1(t, S) - G_1(t, S_1)\| &= \| -((\beta_1 k_1 + \beta_2 k_2 + \lambda k_3 + \mu + \psi))(S(t) - S_1(t)) \\
 &= (\mu + \psi) \|S - S_1\| + \beta_1 I + \beta_2 D + \lambda P \|S - S_1\|. \quad (38)
 \end{aligned}$$

775 Since $I(t)$, $D(t)$ and $P(t)$ are bounded functions, i.e, $\|I\| \leq k_1$, $\|D\| \leq k_2$ and $\|P\| \leq k_3$, by
776 the property of norm functions, the above inequality (38) can be written as

$$\|G_1(t, S) - G_1(t, S_1)\| \leq \eta_1 \|S(t) - S_1(t)\|, \quad (39)$$

778 where $\eta_1 = \beta_1 k_1 + \beta_2 k_2 + \lambda k_3 + \mu + \psi$. Hence for G_1 the Lipschitz condition is obtained and
779 if an additionally $0 \leq \beta_1 k_1 + \beta_2 k_2 + \lambda k_3 + \mu + \psi < 1$, we obtain a contraction. The Lipschitz
780 condition for the other kernels are

$$\left. \begin{aligned}
 \|G_2(t, E) - G_2(t, E_1)\| &\leq \eta_2 \|E(t) - E_1(t)\|, \\
 \|G_3(t, I) - G_3(t, I_1)\| &\leq \eta_3 \|I(t) - I_1(t)\|, \\
 \|G_4(t, R) - G_4(t, R_1)\| &\leq \eta_4 \|R(t) - R_1(t)\|, \\
 \|G_5(t, D) - G_5(t, D_1)\| &\leq \eta_5 \|D(t) - D_1(t)\|, \\
 \|G_6(t, P) - G_6(t, P_1)\| &\leq \eta_6 \|P(t) - P_1(t)\|,
 \end{aligned} \right\} \quad (40)$$

781

782

□

783 Recursively, the expression in (37) can be written as

$$\left. \begin{aligned}
 S_n(t) - S(0) &= \frac{1}{\Gamma(\alpha)} \int_0^t (t - \chi)^{\alpha-1} G_1(\chi, S_{n-1}) d\chi, \\
 E_n(t) - E(0) &= \frac{1}{\Gamma(\alpha)} \int_0^t (t - \chi)^{\alpha-1} G_2(\chi, E_{n-1}) d\chi, \\
 I_n(t) - I(0) &= \frac{1}{\Gamma(\alpha)} \int_0^t (t - \chi)^{\alpha-1} G_3(\chi, I_{n-1}) d\chi, \\
 R_n(t) - R(0) &= \frac{1}{\Gamma(\alpha)} \int_0^t (t - \chi)^{\alpha-1} G_4(\chi, R_{n-1}) d\chi, \\
 D_n(t) - D(0) &= \frac{1}{\Gamma(\alpha)} \int_0^t (t - \chi)^{\alpha-1} G_5(\chi, D_{n-1}) d\chi, \\
 P_n(t) - P(0) &= \frac{1}{\Gamma(\alpha)} \int_0^t (t - \chi)^{\alpha-1} G_6(\chi, P_{n-1}) d\chi,
 \end{aligned} \right\} \quad (41)$$

784

785 The difference between successive terms of system (36) in recursive form is given below:

$$\left. \begin{aligned}
 \phi_{1n} &= S_n(t) - S_{n-1}(t) \\
 &= \frac{1}{\Gamma(\alpha)} \int_0^t (t - \chi)^{\alpha-1} (G_1(\chi, S_{n-1}) - G_1(\chi, S_{n-2})) d\chi, \\
 \phi_{2n} &= E_n(t) - E_{n-1}(t) \\
 &= \frac{1}{\Gamma(\alpha)} \int_0^t (t - \chi)^{\alpha-1} (G_2(\chi, E_{n-1}) - G_2(\chi, E_{n-2})) d\chi, \\
 \phi_{3n} &= I_n(t) - I_{n-1}(t) \\
 &= \frac{1}{\Gamma(\alpha)} \int_0^t (t - \chi)^{\alpha-1} (G_3(\chi, I_{n-1}) - G_3(\chi, I_{n-2})) d\chi, \\
 \phi_{4n} &= R_n(t) - R_{n-1}(t) \\
 &= \frac{1}{\Gamma(\alpha)} \int_0^t (t - \chi)^{\alpha-1} (G_4(\chi, R_{n-1}) - G_4(\chi, R_{n-2})) d\chi, \\
 \phi_{5n} &= D_n(t) - D_{n-1}(t) \\
 &= \frac{1}{\Gamma(\alpha)} \int_0^t (t - \chi)^{\alpha-1} (G_5(\chi, D_{n-1}) - G_5(\chi, D_{n-2})) d\chi, \\
 \phi_{6n} &= P_n(t) - P_{n-1}(t) \\
 &= \frac{1}{\Gamma(\alpha)} \int_0^t (t - \chi)^{\alpha-1} (G_6(\chi, P_{n-1}) - G_6(\chi, P_{n-2})) d\chi,
 \end{aligned} \right\} \quad (42)$$

786

787 with the initial conditions $S_0(t) = S(0)$, $E_0(t) = E(0)$, $I_0(t) = I$, $R_0(t) = R(0)$, $D_0(t) = D(0)$

788 and $P_0(t) = P_0$. Taking the norm of the first equation of (42), we obtain

$$\|\phi_{1n}(t)\| = \|S_n(t) - S_{n-1}(t)\|$$

$$\begin{aligned}
&= \left\| \frac{1}{\Gamma(\alpha)} \int_0^t (t-\chi)^{\alpha-1} (G_1(\chi, S_{n-1}) - G_1(\chi, S_{n-2})) d\chi \right\| \\
&\leq \frac{1}{\Gamma(\alpha)} \left\| \int_0^t (t-\chi)^{\alpha-1} (G_1(\chi, S_{n-1}) - G_1(\chi, S_{n-2})) d\chi \right\|.
\end{aligned} \tag{43}$$

Applying the Lipschitz condition (39) one gets

$$\|S_n(t) - S_{n-1}(t)\| \leq \frac{1}{\Gamma(\alpha)} \eta_1 \int_0^t (t-\chi)^{\alpha-1} \|S_{n-1} - S_{n-2}\| d\chi. \tag{44}$$

Thus, we have

$$\|\phi_{1n}(t)\| \leq \frac{1}{\Gamma(\alpha)} \eta_1 \int_0^t (t-\chi)^{\alpha-1} \|\phi_{1n}(t)\| d\chi. \tag{45}$$

Similarly, for the remainder of the equations in system (2) we have

$$\left. \begin{aligned}
\|\phi_{2n}(t)\| &\leq \frac{1}{\Gamma(\alpha)} \eta_2 \int_0^t (t-\chi)^{\alpha-1} \|\phi_{2n}(t)\| d\chi, \\
\|\phi_{3n}(t)\| &\leq \frac{1}{\Gamma(\alpha)} \eta_3 \int_0^t (t-\chi)^{\alpha-1} \|\phi_{3n}(t)\| d\chi, \\
\|\phi_{4n}(t)\| &\leq \frac{1}{\Gamma(\alpha)} \eta_4 \int_0^t (t-\chi)^{\alpha-1} \|\phi_{4n}(t)\| d\chi, \\
\|\phi_{5n}(t)\| &\leq \frac{1}{\Gamma(\alpha)} \eta_5 \int_0^t (t-\chi)^{\alpha-1} \|\phi_{5n}(t)\| d\chi, \\
\|\phi_{6n}(t)\| &\leq \frac{1}{\Gamma(\alpha)} \eta_6 \int_0^t (t-\chi)^{\alpha-1} \|\phi_{6n}(t)\| d\chi,
\end{aligned} \right\} \tag{46}$$

From (46) one can write

$$\left. \begin{aligned}
S_n(t) &= \sum_{i=1}^n \phi_{1i}(t), & E_n(t) &= \sum_{i=1}^n \phi_{2i}(t), & I_n(t) &= \sum_{i=1}^n \phi_{3i}(t), \\
R_n(t) &= \sum_{i=1}^n \phi_{4i}(t), & D_n(t) &= \sum_{i=1}^n \phi_{5i}(t), & P_n(t) &= \sum_{i=1}^n \phi_{6i}(t),
\end{aligned} \right\} \tag{47}$$

Now, we claim the following result which guaranteed the uniqueness of solution of model (2).

Theorem 5.2. *The proposed fractional epidemic model (2) has a unique solution for $t \in [0, T]$ if the following inequality holds*

$$\frac{1}{\Gamma(\alpha)} b^\alpha \eta_i < 1, \quad i = 1, 2, \dots, 7. \tag{48}$$

Proof. Earlier we have shown that the kernels conditions given in Eqs. (39) and (40) holds.

Thus by considering the Eqs. (46) and (48), and by applying the recursive technique we

obtained the succeeding results as below:

$$\left. \begin{aligned}
\|\phi_{1n}(t)\| &\leq \|S_0(t)\| \left[\frac{1}{\Gamma(\alpha)} b^\alpha \eta_1 \right]^n, & \|\phi_{2n}(t)\| &\leq \|E_0(t)\| \left[\frac{1}{\Gamma(\alpha)} b^\alpha \eta_2 \right]^n, \\
\|\phi_{3n}(t)\| &\leq \|I_0(t)\| \left[\frac{1}{\Gamma(\alpha)} b^\alpha \eta_3 \right]^n, \\
\|\phi_{4n}(t)\| &\leq \|R_0(t)\| \left[\frac{1}{\Gamma(\alpha)} b^\alpha \eta_4 \right]^n, & \|\phi_{5n}(t)\| &\leq \|D_0(t)\| \left[\frac{1}{\Gamma(\alpha)} b^\alpha \eta_5 \right]^n, \\
\|\phi_{6n}(t)\| &\leq \|P_0(t)\| \left[\frac{1}{\Gamma(\alpha)} b^\alpha \eta_6 \right]^n,
\end{aligned} \right\} \tag{49}$$

806 Therefore, the above mentioned sequences exist and satisfy $\|\phi_{1n}(t)\| \rightarrow 0$, $\|\phi_{2n}(t)\| \rightarrow 0$,
807 $\|\phi_{3n}(t)\| \rightarrow 0$, $\|\phi_{4n}(t)\| \rightarrow 0$, $\|\phi_{5n}(t)\| \rightarrow 0$, and $\|\phi_{6n}(t)\| \rightarrow 0$. Furthermore, from Eq. (49) and
808 employing the triangle inequality for any k , we one gets

$$\left. \begin{aligned}
\|S_{n+k}(t) - S_n(t)\| &\leq \sum_{j=n+1}^{n+k} T_1^j = \frac{T_1^{n+1} - T_1^{n+k+1}}{1 - T_1}, \\
\|E_{n+k}(t) - E_n(t)\| &\leq \sum_{j=n+1}^{n+k} T_2^j = \frac{T_2^{n+1} - T_2^{n+k+1}}{1 - T_2}, \\
\|I_{n+k}(t) - I_n(t)\| &\leq \sum_{j=n+1}^{n+k} T_3^j = \frac{T_3^{n+1} - T_3^{n+k+1}}{1 - T_3}, \\
\|R_{n+k}(t) - R_n(t)\| &\leq \sum_{j=n+1}^{n+k} T_4^j = \frac{T_4^{n+1} - T_4^{n+k+1}}{1 - T_4}, \\
\|D_{n+k}(t) - D_n(t)\| &\leq \sum_{j=n+1}^{n+k} T_5^j = \frac{T_5^{n+1} - T_5^{n+k+1}}{1 - T_5}, \\
\|P_{n+k}(t) - P_n(t)\| &\leq \sum_{j=n+1}^{n+k} T_6^j = \frac{T_6^{n+1} - T_6^{n+k+1}}{1 - T_6},
\end{aligned} \right\} \quad (50)$$

810 where $T_i = \frac{1}{\Gamma(q)} b^q \eta_i < 1$ by hypothesis. Therefore, S_n , E_n , I_n , R_n , D_n and P_n are regarded as
811 Cauchy sequences in the Banach space $B(J)$. Hence they are uniformly convergent as described
812 in [52]. Applying the limit theory on Eq. (41) when $n \rightarrow \infty$ affirms that the limit of these
813 sequences is the unique solution of system (2). Ultimately, the existence of a unique solution
814 for system (2) has been achieved. \square

815 We now demonstrate the positivity of solutions for all $t \geq 0$. To prove positivity and bounded-
816 ness of solutions, we need the following Generalized Mean Value Theorem in [?] and corollary.

817 **Lemma 1.** *Suppose that $f(x) \in C[a, b]$ and $D_{t_0}^\alpha f(x) \in C[a, b]$, for $0 < \alpha \leq 1$, then we have*

$$818 \quad f(x) = f(a) + \frac{1}{\Gamma(\alpha)} (D_{t_0}^\alpha f)(\xi)(x - a)^\alpha \quad (51)$$

819 *with $a \leq \xi x$, $\forall x \in (a, b]$ and $\Gamma(\cdot)$ is the gamma function.*

820 **Corollary 1.** *Suppose that $f(x) \in C[a, b]$ and $D_{t_0}^\alpha f(x) \in C(a, b]$, for $0 < \alpha \leq 1$. If $D_{t_0}^\alpha f(x) \geq 0$,
821 $\forall x \in (a, b)$, then $f(x)$ is non-decreasing for each $x \in [a, b]$. If $D_{t_0}^\alpha f(x) \leq 0$, $\forall x \in (a, b)$, then
822 $f(x)$ is non-increasing for each $x \in [a, b]$.*

823 We now prove that the non-negative orthant \mathbb{R}_+^6 is positively invariant region. To do this,
824 we need to show that on each hyperplane bounding the non-negative orthant, the vector field

825 points to \mathbb{R}_+^6 . From model (2), one gets:

$$826 \quad D_{t_0}^\alpha S(t)|_{S=0} = \Lambda^\alpha \geq 0, \quad (52)$$

$$827 \quad D_{t_0}^\alpha E(t)|_{E=0} = \psi^\alpha S(t) \geq 0, \quad (53)$$

$$828 \quad D_{t_0}^\alpha I(t)|_{I=0} = (\beta_1^\alpha I(t) + \beta_2^\alpha D(t) + \lambda^\alpha P(t))(S(t) + \gamma^\alpha E(t)) \geq 0, \quad (54)$$

$$829 \quad D_{t_0}^\alpha R(t)|_{R=0} = \sigma^\alpha I(t) \geq 0, \quad (55)$$

$$830 \quad D_{t_0}^\alpha D(t)|_{D=0} = (\mu^\alpha + \delta^\alpha)I(t) \geq 0, \quad (56)$$

$$831 \quad D_{t_0}^\alpha P(t)|_{P=0} = \rho^\alpha I(t) + \theta^\alpha D(t) \geq 0, \quad (57)$$

832 Thus, by Corollary 1, the solution of model (2) are always positive for $t \geq 0$. We now demon-
833 strate that all solutions of model (2) are bounded above for all $t \geq 0$. To do this, we need the
834 following Lemma 2 and Lemma 3.

835 **Lemma 2.** (see [53]). Let $\alpha > 0$, $n-1 < \alpha < n - \mathbb{N}$. Suppose that $f(t), f'(t), \dots, f^{(n-1)}(t)$ are
836 continuous on $[t_0, \infty)$ and the exponential order and that $D_{t_0}^\alpha f(t)$ is piecewise continuous on
837 $[t_0, \infty)$. Then

$$838 \quad \mathcal{L}\{D_{t_0}^\alpha f(t)\} = s^\alpha \mathcal{F}(s) - \sum_{k=0}^{n-1} s^{\alpha-k-1} f^{(k)}(t_0) \quad (58)$$

839 where $\mathcal{F}(s) = \mathcal{L}\{f(t)\}$.

840 **Lemma 3.** (see [54]). Let \mathbb{C} be the complex plane. For any $\alpha > 0$ $\beta > 0$, and $A \in \mathbb{C}^{n \times n}$, we
841 have

$$842 \quad \mathcal{L}\{t^{\beta-1} E_{\alpha,\beta}(At^\alpha)\} = s^{\alpha-\beta} (s^\alpha - A)^{-1},$$

843 for $\mathcal{R}s > \|A\|^\frac{1}{\alpha}$, where $\mathcal{R}s$ represents the real part of the complex number s , and $E_{\alpha,\beta}$ is the
844 Mittag-Leffler function [55].

845 Since all solutions of model system (2) have been shown to be positively invariant and have a
846 lower bound zero (52)-(57), we now proceed to demonstrate that these solutions are bounded
847 above. By summing all equations of system (2) one gets:

$$848 \quad \begin{aligned} D_{t_0}^\alpha N(t) &= \Lambda^\alpha - \mu^\alpha N(t) - \epsilon^\alpha D(t) - (\tau^\alpha + \eta^\alpha)P(t) \\ &\leq \Lambda^\alpha - \mu^\alpha N(t). \end{aligned} \quad (59)$$

849 Taking the Laplace transform of (59) leads to:

$$850 \quad s^\alpha \mathcal{L}(N(t)) - s^{\alpha-1} N(0) \leq \frac{\Lambda^\alpha}{s} - \mu^\alpha \mathcal{L}(N(t)). \quad (60)$$

851 Combining like terms and arranging leads to

$$\begin{aligned}
 \mathcal{L}(N(t)) &\leq \Lambda^\alpha \frac{s^{-1}}{s^\alpha + \mu^\alpha} + N(0) \frac{s^{\alpha-1}}{s^\alpha + \mu^\alpha} \\
 &= \Lambda^\alpha \frac{s^{\alpha-(1+\alpha)}}{s^\alpha + \mu^\alpha} + N(0) \frac{s^{\alpha-1}}{s^\alpha + \mu^\alpha}.
 \end{aligned}
 \tag{61}$$

853 Applying the inverse Laplace transform leads to

$$\begin{aligned}
 N(t) &\leq \mathcal{L}^{-1} \left\{ \Lambda^\alpha \frac{s^{-1}}{s^\alpha + \mu^\alpha} + N(0) \frac{s^{\alpha-1}}{s^\alpha + \mu^\alpha} \right\} + \mathcal{L}^{-1} \left\{ N(0) \frac{s^{\alpha-1}}{s^\alpha + \mu^\alpha} \right\} \\
 &\leq \Lambda^\alpha t^\alpha E_{\alpha, \alpha+1}(-\mu t^\alpha) + N(0) E_{\alpha, 1}(-\mu t^\alpha) \\
 &\leq \frac{\Lambda^v}{\mu^\alpha} \mu^\alpha t^\alpha E_{\alpha, \alpha+1}(-\mu t^\alpha) + N(0) E_{\alpha, 1}(-\mu t^\alpha) \\
 &\leq \max \left\{ \frac{\Lambda^\alpha}{\mu^\alpha}, N(0) \right\} (\mu^\alpha t^\alpha E_{\alpha, \alpha+1}(-\mu t^\alpha) + E_{\alpha, 1}(-\mu t^\alpha)) \\
 &= \frac{C}{\Gamma(1)} = C,
 \end{aligned}
 \tag{62}$$

854 where $C = \max \left\{ \frac{\Lambda^\alpha}{\mu^\alpha}, N(0) \right\}$. Thus, $N(t)$ is bounded from above. This completes the proof of
 855 Theorem (3.1).
 856